Received: 26 April 2024 | Accepted: 25 June 2024

DOI: 10.1002/biof.2107

RESEARCH ARTICLE

Biofactors WILEY

Berberine chloride loaded nano-PEGylated liposomes attenuates imidacloprid-induced neurotoxicity by inhibiting NLRP3/Caspase-1/GSDMD-mediated pyroptosis

Walaa Bayoumie El Gazzar[1,2] | **Amina A. Farag**[3] | **Mohamed Samir**[4,5] | **Heba Bayoumi**[6] | **Heba S. Youssef**[7] | **Yasmin Mohammed Marei**[2] | **Shimaa K. Mohamed**[8] | **Azza M. Marei**[9] | **Reham M. Abdelfatah**[10] | **Manal Moustafa Mahmoud**[11] | **Elshaimaa Ahmed Fahmy Aboelkomsan**[12] | **Eman Kamel M. Khalfallah**[13] | **Hala Magdy Anwer**[7]

[1]Department of Anatomy, Physiology and Biochemistry, Faculty of Medicine, The Hashemite University, Zarqa, Jordan

[2]Department of Medical Biochemistry and Molecular biology, Faculty of Medicine, Benha University, Benha City, Qalyubia, Egypt

[3]Department of Forensic Medicine and Clinical Toxicology, Faculty of Medicine, Benha University, Benha City, Qalyubia, Egypt

[4]Department of Zoonoses, Faculty of Veterinary Medicine, Zagazig University, Zagazig, Sharqia, Egypt

[5]School of Science, Faculty of Engineering and Science, University of Greenwich, Kent, UK

[6]Department of Histology and Cell Biology, Faculty of Medicine, Benha University, Benha City, Egypt

[7]Department of Physiology, Faculty of Medicine, Benha University, Benha City, Qalyubia, Egypt

[8]Department of Pharmacology and Toxicology, Faculty of Pharmacy, Helwan University, Cairo, Egypt

[9]Department of Zoology, Faculty of Science, Benha University, Benha City, Qalyubia, Egypt

[10]Department of Pesticides, Faculty of Agriculture, Mansoura University, Mansoura, Egypt

[11]Department of Medical Physiology, Faculty of Medicine, Cairo University, Cairo, Egypt

[12]Department of Pathology, School of Medicine, New Giza University (NGU), Giza, Egypt

[13]Department of Biochemistry, Toxicology and Feed Deficiency, Animal Health Research Institute (AHRI), Agricultural Research Center (ARC), Dokki, Giza, Egypt

Correspondence
Walaa Bayoumie El Gazzar, Department of Anatomy, Physiology and Biochemistry, Faculty of Medicine, The Hashemite University, P.O. Box 330127, Zarqa, 13133, Jordan.
Email: wallagazzar@hu.edu.jo; bioch_2004@yahoo.com

Abstract

Concerns have been expressed about imidacloprid (IMI), one of the most often used pesticides, and its potential neurotoxicity to non-target organisms. Chronic neuroinflammation is central to the pathology of several neurodegenerative disorders. Hence, exploring the molecular mechanism by which IMI would trigger neuroinflammation is particularly important. This study examined the neurotoxic effects of oral administration of IMI (45 mg/kg/day for 30 days) and the potential neuroprotective effect of berberine (Ber) chloride loaded nano-PEGylated liposomes (Ber-Lip) (10 mg/kg, intravenously every other day for 30 days) using laboratory rat. The histopathological changes, anti-oxidant and oxidative stress markers (GSH, SOD, and MDA),

Abbreviations: AD, Alzheimer's disease; BBB, blood–brain barrier; Ber, berberine; GSDMD, gasdermin D; GSH, reduced glutathione; IL1β, interleukin-1β; IMI, imidacloprid; MDA, malondialdehyde; nAChRs, nicotinic acetylcholine receptors; NEP, neprilysin; NNs, neonicotinoids; SOD, superoxide dismutase; TNF-α, tumor necrosis factor.

proinflammatory cytokines (IL1β and TNF-α), microglia phenotype markers (CD86 and iNOS for M1; CD163 for M2), the canonical pyroptotic pathway markers (NLRP3, caspase-1, GSDMD, and IL-18) and Alzheimer's disease markers (Neprilysin and beta amyloid [Aβ] deposits) were assessed. Oral administration of IMI resulted in apparent cerebellar histopathological alterations, oxidative stress, predominance of M1 microglia phenotype, significantly upregulated NLRP3, *caspase-1*, *GSDMD*, *IL-18* and Aβ deposits and significantly decreased Neprilysin expression. Berberine reduced the IMI-induced aberrations in the measured parameters and improved the IMI-induced histopathological and ultrastructure alterations brought on by IMI. This study highlights the IMI neurotoxic effect and its potential contribution to the development of Alzheimer's disease and displayed the neuroprotective effect of Ber-Lip.

KEYWORDS

Alzheimer's disease, berberine, cerebellum, imidacloprid, nano-PEGylated liposomes, neurotoxicity, pyroptosis

1 | INTRODUCTION

One of the neonicotinoids (NNs), a developing class of synthetic pesticides with the biggest market share globally, is imidacloprid (IMI).[1] NNs were created to have a structure that is comparable to nicotine's, and they share this substance's ability to affect the cholinergic neurotransmitter system. The NN pesticides exert their neurotoxic effects on target insects through their agonistic action on the nicotinic acetylcholine receptors (nAChRs), which are broadly dispersed in the CNS of these invertebrates. The hypothesis that this group of insecticides has a low affinity for the mammalian nAChRs and a limited blood–brain barrier (BBB) penetration has prompted the idea that these insecticides, in comparison to earlier insecticides, are substantially less hazardous for this group of vertebrates. However, in recent decades, several NNs' detrimental effects have been documented on non-target organisms' health, which has prompted re-evaluation to the presumed minimal toxicity of these insecticides.[2] Several recent studies have revealed that these insecticides can persist in the environment for times ranging from 1 day to almost 19 years. As a result, people are continually subjected to these pesticides, which can also be absorbed by food or drinking water, by inhalation, or through skin contact, leading to cumulative evidence of long-term exposure to IMI.[3] Exposure of different animal species to this group of pesticides has been connected to mutagenic, immunotoxic and neurotoxic effects, as well as endocrine disturbance and reproductive toxicity. Recently, the presence of NNs in rodent brain tissue and the neurological symptoms seen in humans provide a substantial proof that these insecticides have the ability to penetrate the BBB and reach the CNS. Once inside the brain, the NNs have been demonstrated to exert significant neurotoxic effects that are either directly or indirectly linked to their action on the nAChR receptors.[2]

One of the processes through which NNs might exert their toxicity is oxidative stress. When the body's antioxidant system is unable to effectively scavenge reactive oxygen or nitrogen species, oxidative stress results.[4] Free radical overproduction results in significant degradation of proteins, the breakdown of DNA, and the peroxidation of lipids, which all contribute to cellular dysfunction.[5] The brain tends to be vulnerable to oxidative damage due to its high lipid content, rapid oxygen consumption, and low capacity for antioxidants.[4]

Additionally, while the inflammatory process is crucial for the immune system's ability to combat noxious threats, when it is out of control or persists for an extended period of time, it can cause progressive damage to the tissues. The release of cytokines, chemokines, and secondary messengers controls the inflammatory response in the CNS.[2] In the CNS, astrocytes and microglia produce and release the majority of these mediators.[6] Therefore, the microglial cells are activated when an insult occurs as a result of the activity of neurotoxic chemicals such as pesticides. A number of morphological and functional alterations to the microglia occur when these cells are activated. There are two primary polarization states or phenotypes that exhibit opposing traits: the

M1 cytotoxic-proinflammatory phenotype and the M2 cytoprotective-anti-inflammatory phenotype.[2] The M1, or cytotoxic microglia, secrete proinflammatory cytokines that increase tissue damage and compromise neuroprotection.[7] In contrast, the synthesis of growth factors and anti-inflammatory cytokines, which promote tissue regeneration, is associated with activation of the M2 phenotype.[8] The M1 cytotoxic phenotype is promoted by exposure to NN pesticides, which may increase neurotoxicity by causing excessive production of proinflammatory cytokines including IL1β and TNF-α.[2]

Inflammasomes are cytoplasmic multiprotein complexes made up of a sensor protein, inflammatory caspases, and occasionally, an adapter protein connecting the two. They can be induced by a variety of endogenous and exogenous stimuli, leading to enzymatic activation of canonical caspase-1, noncanonical caspase-11 (or the humans equivalents caspase-4 and caspase-5 in humans) or caspase-8, resulting in secretion of IL1β and IL-18, as well as apoptotic and pyroptotic cell death.[9] Inflammasome activation was first discovered in myeloid cells, including microglia, neutrophil, and dendritic cell.[10] Up-to-date, several inflammasomes have been described, including NLRP3, NLRP1, AIM2, and NLRC4. The NLRP3 inflammasome comprises the sensor molecule NLRP3, the adaptor protein ASC, and pro-caspase-1 which is activated to caspase-1 and then proceeds to cleave the cytokines precursors pro-IL1β and pro-IL-18 into mature IL1β and IL-18.[11] In addition, active caspase-1 also cleaves and activates gasdermin D (GSDMD), the effector in pyroptosis.[8] Pyroptosis is a distinct form of programmed cell death connected to inflammation. Pyroptosis, as opposed to apoptosis, is triggered by inflammasomes and is a key component of disorders related to inflammation.[12] The cleaved GSDMD creates plasma membrane holes and encourages the release of additional proinflammatory cytokines, which increase synaptic loss and neuronal death.[6] Inflammasome-mediated-inflammation and pyroptosis promote neurodegeneration. Clear evidence of enhanced pyroptosis-related proteins activity in common neurodegenerative diseases has coincided with abnormal aggregation of pathological proteins (such as Aβ, tau, α-synuclein), making pyroptosis an attractive direction for the recent study of neurodegenerative diseases.[13,14]

Neprilysin (NEP, CD10, neutral endopeptidase) is a membrane-bound metallopeptidase that has a wide range of physiological applications and substrates. It is an important neuropeptidase and amyloid-degrading enzyme which makes NEP a therapeutic target in Alzheimer's disease (AD).[15,16] Microglia and astrocytes, the primary cellular effectors of innate immunity in the CNS, express the highest levels of NEP expression in the brain, implying that NEP expression and function may be modulated by neuroinflammation.[17] While the cerebellum is one of the brain areas most often disregarded in the context of AD with few biochemical, molecular and histological observations reported both in AD patients and mice models, there has been a recent surge in interest in cerebellar lesions due to their potential association with cognitive alterations.[18] Therefore, we focused to detect the biochemical, molecular, and histological alterations in the cerebellum tissue associated with IMI administration.

Berberine (Ber), a natural isoquinoline alkaloid compound, has a variety of medicinal effects, such as antibacterial, antiviral, anti-inflammatory, anticancer, hypoglycemic, and lipid-regulating properites.[19,20] Accumulating evidence indicate that Ber may act as a promising anti-neurodegenerative agent,[21] but the molecular mechanisms that underlie its neuroprotective effect are not well clarified. Beside the beneficial effects of Ber, its applications have been limited by its poor aqueous solubility, minimal absorption, and low bioavailability. To overcome these constraints, different types of nanocarriers have been used for encapsulation of Ber.[22] In this study, Ber loaded lipid-based nanocarriers (liposomes) were utilized to enhance its solubility and bioavailability.

The present study aimed to determine the impact of IMI oral exposure on cerebellar microglial polarization, pyroptosis and Neprilysin expression in order to clarify the molecular mechanisms underlie its potential neurotoxic effect in male rats. Furthermore, we made an effort to ascertain whether Ber Chloride loaded nano-PEGylated liposomes treatment could efficiently alleviate any anticipated neuronal damage from exposure to IMI.

2 | MATERIALS AND METHODS

2.1 | Preparation of long-circulating Ber chloride loaded nano-PEGylated liposomes (Ber-Lip)

Ber-Lip were prepared using solvent injection method as previously reported.[23–25] In brief, phospholipon 90G, cholesterol, polyethylene glycol (PEG), and Ber (13:3:1:0.2 wt/wt) were dissolved in 5 mL of absolute ethanol to form the organic phase and kept at 60–70°C. The aqueous phase was prepared by dissolving sucrose in deionized water to form a 9% w/v solution and kept at 60–70°C under stirring (700 rpm). The preheated organic phase was injected into the prepared aqueous phase using a syringe (23G) into a closed system. After the completion of the injection process, the obtained suspension was kept under stirring at 60–70°C for 20 min to allow the evaporation of ethanol. The resultant liposomal

suspension was kept at 4°C until further investigations. The liposomal systems were evaluated using mean particle diameter, zeta potential, transmission electron microscopy, and in vitro drug release study.

The entrapment efficiency of the prepared Ber chloride-loaded PEGylated liposomal systems was determined via the lysis method as previously reported with minor modifications.[26] Simply, the liposomal suspension was centrifuged for 60 min at 15,000 rpm using a cooling centrifuge (Hermle, Essen, Germany). The pellet was resuspended in a 9% sucrose solution and twice washed after the unentrapped Ber chloride was removed. To lyse liposomal systems, a mixture of liposomes and acetonitrile (1:4) was exposed to vortexing for 5 min and sonication for 20 min. Next, the mixture underwent a 10,000-rpm centrifugation. Using a standard curve, the amount of Ber chloride in the supernatant was measured spectrophotometrically at 346 nm (Shimadzu, Kyoto, Japan). Entrapment efficiency percentage (EE%) was determined using the following equation: EE% = Xs / Xt × 100 where Xs is the amount of Ber determined after the lysis of liposomes and Xt is Ber chloride total amount.

In vitro release of Ber chloride in the form of liposomes was also examined, as previously reported.[23] In the sample compartment of a homemade Franz diffusion cell, an aliquot of Ber-Lip was put. The release media, which was put in the reservoir compartment, was PBS with a pH of 7.4. The two compartments were separated by a nitrocellulose membrane with a molecular weight cut off of 12,000–14,000 Da. System speed and temperature were kept at 50–60 rpm and 37°C, respectively. To quantify Ber chloride using a standard curve, 2 mL of the reservoir medium were taken at regular intervals and placed through UV analysis at 346 nm. The reservoir compartment was filled with a similar volume of release medium that was kept at 37°C.

2.2 | Animals

Twenty-eight adult male albino rats (weighing 150–180 g) were obtained from the Faculty of Agriculture, Benha University, Moshtohor, Egypt. Rats were categorized into four groups of 7, and each group of rats was housed in separate cages kept at 23°C ± 2°C with a relative humidity of (45% ± 5%), and 12/12 h light and dark cycles. Additionally, all rats were provided free access to water ad libitum as well as food. Prior to the trial, all rats were acclimated to the laboratory environment for 1 week. The research adhered to the guidelines for the care and use of laboratory animals,[27] as well as approved by the Faculty of Medicine's Research Ethics Committee, Benha University, Egypt (Approval No. RC: 41-1-2024). Figure 1 is a schematic representation summarizing the experimental procedure.

2.3 | Chemicals

Imidacloprid (CAS No. 138261-41-3) was purchased from Bayer Cropscience, Germany. Berberine chloride and cholesterol were obtained from Sigma–Aldrich (Sigma, St. Louis, MO). Phosopholipon 90G was purchased from Lipoid GmbH (Ludwigshafen, Germany).

2.4 | Study design

The animals were divided into the following groups:

Group I (control group; n = 7): This group received 1 mL of oral corn oil (solvent of IMI) once daily for 30 days.

Group II (Ber-Lip group; n = 7): This group received 10 mg/kg b wt. Ber-Lip intravenously every other day for 30 days.

Group III (IMI group; n = 7): This group received 45 mg/kg IMI orally once daily for 30 days. This dose is 1/10 of LD50.[28,29]

Group IV (IMI + Ber-Lip group; n = 7): This group received 45 mg/kg IMI orally once daily and 10 mg/kg Ber-Lip intravenously every other day for 30 days. The animals received the Ber-Lip then 1 h later received IMI. On the 31st day, all rats were euthanized via decapitation following inhalation anesthesia with isoflurane (El Amriya for pharmaceutical industries, Al Amyria, Alexandria) and the cerebellums were dissected.

The two cerebellar hemispheres of each rat were separated. The left hemisphere was used for biochemical and PCR analysis (anterior part for biochemical analysis, and posterior part for PCR analysis). The right hemisphere was used for histopathological and immunohistochemical examination. Two small pieces from the anterior cortical area of each right hemisphere about (1 mm^3) were put in 2.5% solution of glutaraldehyde on 0.1 M phosphate buffer (pH = 7.4) mixed with 4.0% paraformaldehyde as primary fixative for electron microscopy tissue processing. The remaining right hemisphere was immersed in 10% neutral buffered formalin for paraffin blocks preparation.

2.5 | Biochemical analysis

Samples of cerebellar tissues were utilized for the biochemical markers and were rinsed in ice-cold saline before being homogenized with phosphate buffer (pH 6–7) utilizing a mixer mill MM400 (Retsch, Germany).

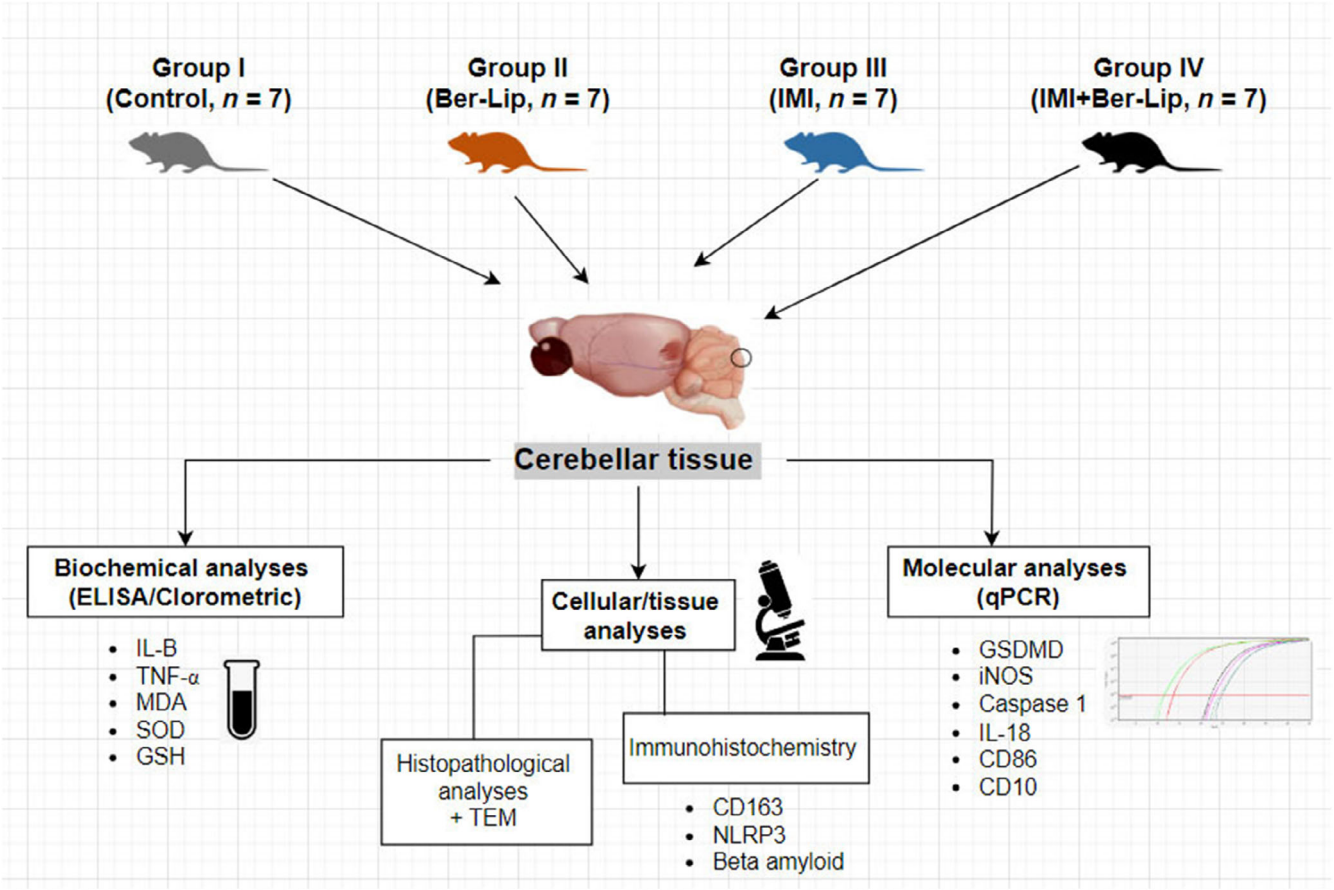

FIGURE 1 Schematic representation of the whole study. Four-groups of rat (7-unit each) were used in the experiment and various pieces of the cerebellar tissue were used for biochemical, tissue, and molecular analyses.

Centrifugation of tissue homogenates was performed for 15 min at 4000 rpm, 4°C. Afterward, the supernatant was utilized to quantitatively assess the following proinflammatory cytokines and oxidative stress markers per the manufacturer: Interleukin-1β (IL1β) utilizing Rat IL-1β quantikine ELISA Kit (Catalog # RLB00; R&D Systems, Minneapolis, MN), tumor necrosis factor (TNF-α) utilizing rat TNF-alpha quantikine ELISA Kit (Catalog #: RTA00; R&D Systems, Minneapolis, MN), reduced glutathione (GSH) (Catalog # GR 25 11; BioDiagnostic, Giza, Egypt), superoxide dismutase (SOD) (Catalog # SD 25 21; BioDiagnostic, Giza, Egypt) and malondialdehyde (MDA) (Catalog # SD 25 29; BioDiagnostic, Giza, Egypt).

2.6 | Quantitative real-time polymerase chain reaction analysis for mRNA gene expression of *GSDMD*, *iNOS*, *casspase-1*, IL-*18*, CD *86*, and CD *10*

Samples of cerebellar tissues utilized for RNA extraction and qPCR were preserved in RNAlater™ stabilization solution (Catalog No: AM7021; Thermo Fisher Scientific, MA) at 10 μL per 1 mg of tissue, then, samples were frozen at −80°C for subsequent RNA extraction and purification.

2.6.1 | Total RNA extraction and reverse transcription

Total RNA extraction from the cerebellar tissue samples was performed using Qiazol lysis reagent (Catalog No: 79306; Qiagen, Hilden, Germany) according to the manufacturer's guidelines. RNA purity and concentration were evaluated utilizing a NanoDrop® ND–1000 spectrophotometer (NanoDrop Technologies; Wilmington, DE). The RNA's reverse transcription (RT) into complementary DNA (cDNA) was performed utilizing the high-capacity cDNA reverse transcription kit (Catalog No: 4368814; Applied Biosystems, Foster City, CA).

2.6.2 | Quantitative real-time PCR

The real-time RT-PCR was performed in a Mx3005P Real-Time PCR System (Agilent Stratagene, Santa Clara,

TABLE 1 Primer sequences utilized for RT-PCR analysis.

Gene name	Primer sequences (5′ → 3′) (F: forward; R: reverse)	Accession number
GSDMD	F: GTGAAGATCGTGGTGAGCC R: GCATGATCCAGAGTAGGGGC	NM_001400994.1
IL-18	F: GCACAGCCTCTCAGTTGGAA R: ACTCATCGTTGTGGGGACAG	NM_019165.2
caspase-1	F: CTCATGGTCTCCAGGAGGGA R: TCCTTGTTTCTCTCCACGGC	NM_012762.3
iNOS	F: ACACAGTGTCGCTGGTTTGA R: AACTCTGCTGTTCTCCGTGG	NM_012611.3
CD86	F: TACTGTGCTTGTGTGTGGGG R: CCCAAGTACATGGTGCAGGT	NM_020081.2
CD10	F: ACACAAACTCTGGGGTGAGC R: CTTAGCCACTGAGGCCAGAC	NM_012608.2
B-actin	F: AACCTTCTTGCAGCTCCTCC R: CCATACCCACCATCACACCC	NM_031144.3

CA) using TOPreal™ qPCR 2X PreMIX (SYBR Green with low ROX) (Catalog No: RT500S, Enzynomics, Korea) following the manufacturer's instructions. The oligonucleotide specific primers were synthesized by Sangon Biotech (Beijing, China), displayed in Table 1. The PCR cycling conditions included an initial denaturation at 95°C for 12 min followed by 40 cycles, each entails denaturation at 95°C for 20 s, annealing at 60°C for 30 s, and extension at 72°C for 30 s. After adjusting for *B-actin* expression, each sample's mRNA expression was determined. The relative expression was computed utilizing the $2^{-\Delta\Delta Ct}$ method.[30] The findings are expressed as the *n*-fold difference relative to controls.

2.7 | Histological study

Cerebellar tissue samples were flushed and fixed in 10% neutral buffered formalin for 72 h. Samples were trimmed and processed in serial grades of ethanol, cleared in xylene, synthetic wax infiltration and embedding into paraplast tissue embedding media. Five-micron thick tissue sections were cut by rotatory microtome, fixed to glass slides and stained by Hematoxylin and Eosin as a general standard histological examination staining method, then examined by experienced histologist in blinded manner. All standard procedures for samples fixation, processing and staining were done according to Bancroft and Layton.[31] Slides were examined blindly on (×400 magnification). Semi-quantitative analysis of cerebellar cortical damage scoring was done in the examined sections regarding Purkinje cells damage/loss, brain matrix edema and glial cells infiltrates. The results were recorded as (−) nil, (+) mild, (++) moderate, and (+++) sever.

2.8 | Immunohistochemical study

According to standard procedures,[32] depraffinized 5-μm thick tissue section were cut and prepared, tissue sections were treated by 3% hydrogen peroxide for 20 min, washed by PBS, then incubated with *anti-CD163* (Cat No: GTX35247, GeneTex, CA; 1:100), *anti NLRP3* (GTX00763–1:100—Genetex Co) and *anti-beta amyloid* (ab201060—Abcam co; 1:1000) overnight at 4°C; washed by PBS followed by incubation with secondary antibody HRP Envision kit (DAKO) 20 min; washing by PBS and incubated with diaminobenzidine (DAB) for 10 min. Washing by PBS then counter staining with hematoxylin, dehydrated and clearing in xylene then cover slipped for microscopic analysis.

2.9 | Microscopic analysis

According to Mohamed et al.,[33] one slide was prepared for each rat. Six random non-overlapping fields (×400 magnification) from cerebellar folia per tissue section of each sample were analyzed for determination of cerebellar cortex damage scoring, mean reactive positive microglial cells for CD163 and relative area percentage of immunohistochemical expression of NLRP3 as well as mean diameter of beta amyloid deposits in immunostained sections. All micrographs and data were obtained by using Full HD microscopic camera operated by Leica application module for tissue sections analysis (Leica Microsystems GmbH, Wetzlar, Germany).

2.10 | Transmission electron microscopic examination

After primary fixation with 2.5% solution of glutaraldehyde on 0.1 M phosphate buffer (pH = 7.4), mixed with 4.0% paraformaldehyde. Fixative was washed away by distilled water three times in 10 min. Then, the samples were post-fixed in 1.0% osmium tetraoxide solution for 2 h. After fixation, the tissue was washed, dehydrated and embedded in fresh resin overnight at 60°C. Ultrathin slices (70–90 nm) were cut using ultra-microtome and stained with double staining technique utilizing an aqueous solution of uranyl acetate followed by aqueous lead citrate. Tissue evaluation of the sections was done at the electron microscopic (Faculty of Agriculture, Mansoura University, Egypt) using (J.E.O.L., JEM-2100; Tokyo, Japan) operated at 80 kV. The protocol was done according to Bozzola.[34]

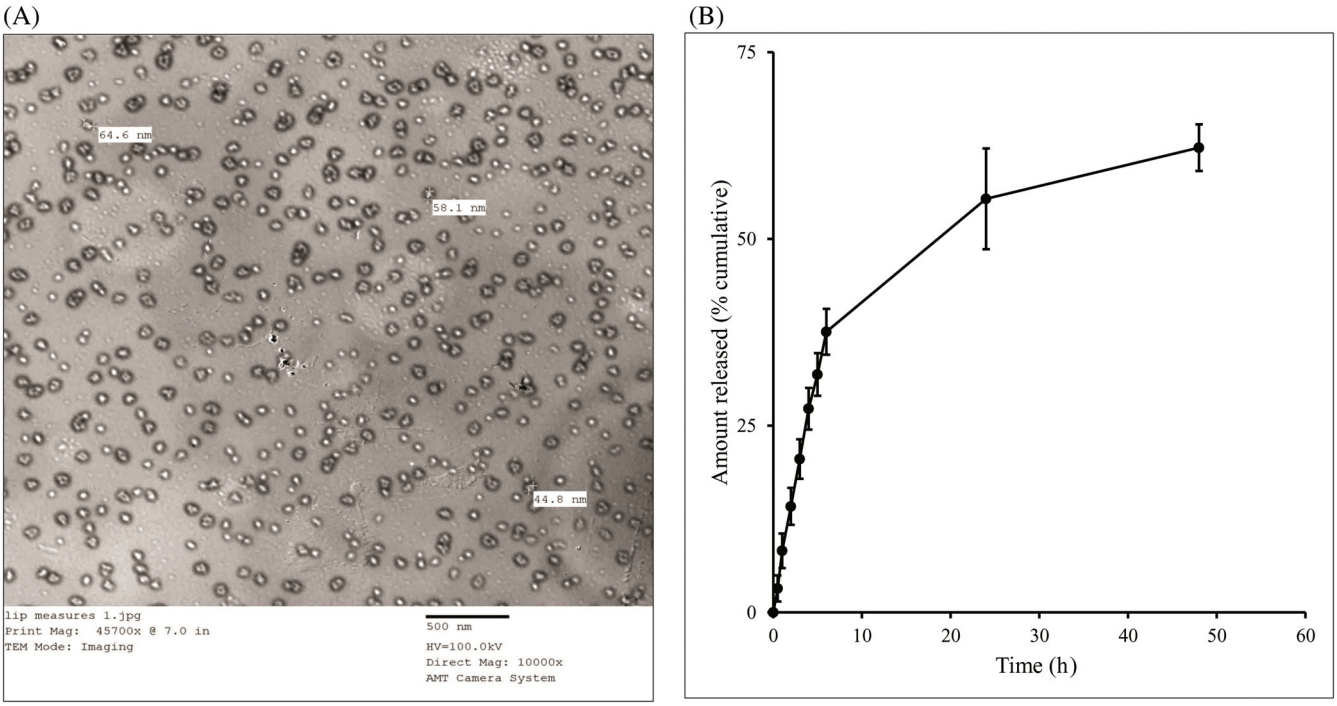

FIGURE 2 Characterization of Ber-Lip. (A) Transmission electron microscopy examination showing the spherical nature of the Ber-Lip. (B) In vitro Ber from Ber-Lip over 48 h.

2.11 | Statistical analysis

To compare the means among various groups for the measured parameters, we first tested the distribution of each variable using Q–Q plots and Shapiro test and then parametric one-way ANOVA was used followed by Duncan's post hoc test. The differences among groups were considered statistically significant if the adjusted *p*-value was <0.05 with the degree of the significance being assessed using the following thresholds *<0.05, **<0.01, ***<0.001. The software graph Pad prism V8[35] was used for performing the statistical analyses and data visualization. To determine the association among various groups, we run a principle component analyses (PCA) based on the measured variables. Data were scaled and centered to ensure equal contribution of each variable to the various components. This analyses and the associated visualization were done using packages ggplot2[36] and ggbiplot[37] in the R software version 4.3.2.

3 | RESULTS

3.1 | Characterization of Ber-Lip suspension

Liposomal particles were analyzed using a Malvern Nano sizer for their particle size distribution and zeta potential. The results obtained revealed particle size distribution and zeta potential of 95.7 ± 3.05 nm and −10.1 ± 0.72 mV, respectively. The polydispersity index was found to be 0.207 indicating a homogeneous particle size distribution. Transmission electron microscopy results confirmed the spherical nature of the Ber-Lip as shown by Jeol JEM-1010 (Tokyo, Japan) in Figure 2A. The entrapment efficiency was determined to be 18.66% ± 1.62%, which is low due to Ber hydrochloride's hydrophilic characteristics. The in vitro release testing revealed the sustained release of Ber over 48 h of the release study. Liposomal systems released about 37% of the loaded amount after 6 h and increased to 55% and 62% after 24 and 48 h, respectively (Figure 2B).

3.2 | Ber-Lip improved cerebellar histopathological changes induced by IMI exposure

As shown in Figure 3i–iv, the control and Ber-Lip groups showed normal three layers of cerebellar cortex including inner dark granule cells layer, middle Purkinje cells layer, and pale outer molecular layer. After 30 days of oral IMI intoxication, Purkinje cells displayed apoptotic features with nuclear pyknosis and cellular shrinkage. Some other cells were completely degenerated with occasional focal loss of neurons. Many vacuolar spaces around cells in molecular layer as well as Purkinje cell layer were

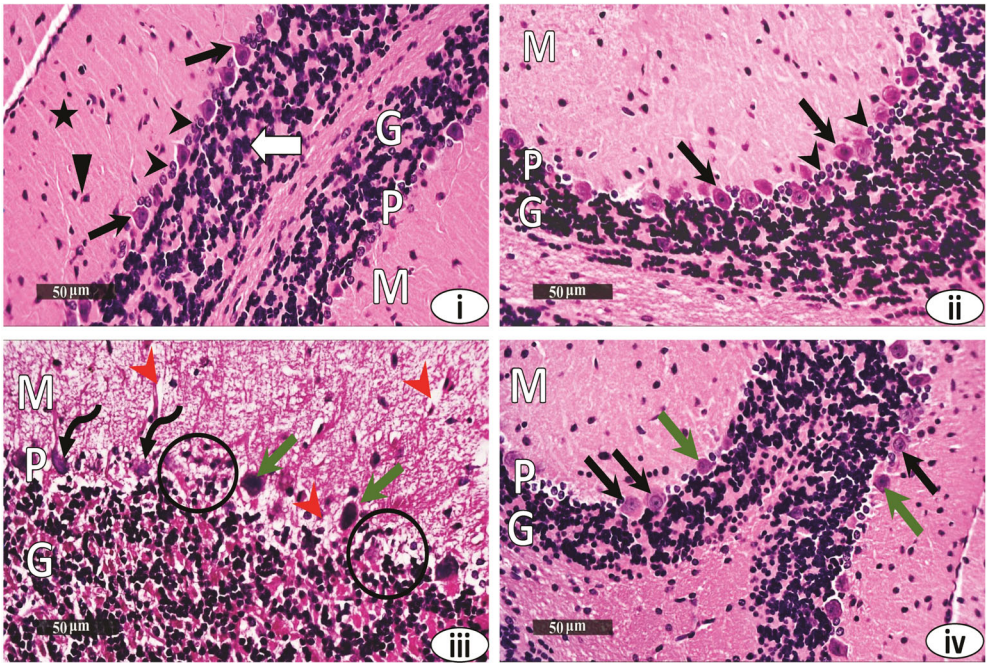

FIGURE 3 Set of micrographs representing cerebellar cortices stained with H&E of different experimental groups: (i) Control group: normal histological morphology, including outer Pale molecular layer (M): long nerve fibers (star) and neuroglial cells (triangle) without abnormal infiltrates, middle Purkinje cells layer (P): normal Purkinje cells (black arrows) with vesicular nuclei and apical processes, surrounded by Bergmann astrocytes (black arrow heads), and inner dark granule cells layer (G): clumps of darkly stained granule cells (thick arrow) with non-cellular cerebellar islands in-between. (ii) Ber-Lip group: well organized morphological features of cerebellar layers without abnormal light microscopic changes records resembling normal controls. (iii) IMI group: many figures of shrunken apoptotic Purkinje neurons (green arrows) with ill distinct cellular details, other cells are completely degenerated (curved arrows), focal loss of neurons with reactive cellular infiltrate (circles) and moderate perineuronal edema, vacuolization of molecular cells layer (red arrow heads). (iv) IMI+ Ber-Lip group: significant protective efficacy with abundant records of apparent intact purkinje cells (black arrow) with occasional sporadic records of degenerative neuronal changes (green arrows). Moreover; almost intact intercellular brain matrix without abnormal vacuolization or abnormal cellular infiltrates (scale bar = 50 µm, magnification = ×400).

obvious. In contrast, co-administration of IMI+ Ber-Lip abolished the toxic effect of IMI. This group showed some intact, protected neurons with occasional sporadic records of degenerative neuronal changes indicating protective effect of Ber-Lip. Results of the semi-quantitative analysis done for the cerebellar cortical damage scoring displayed sever records of Purkinje cell damage as well as moderate peri-neural edema and cellular infiltrate in the IMI group. Ber-Lip reversed theses records in the IMI+ Ber-Lip group with only few records of Purkinje cell damage (Table 2).

3.3 | Ber-Lip improved the cerebellar ultrastructure pathological changes induced by IMI exposure

The TEM examination of the three layers of cerebellar cortices from each group of rats supported the histopathological findings. Examination of control group revealed normal Purkinje cells with characteristic large euchromatic nuclei, normal densely packed small granule cells and myelinated nerve axons in molecular layer as displayed in Figures 4A-i,B-i and 5A-i, respectively. This group also showed normal elongated microglial cells within the neuropil with dark nucleus (Figure 5B-i). The Ber-Lip group showed the same normal ultrastructural morphology (Figures 4A-ii,B-ii and 5A-ii,B-ii).

As expected, IMI intoxication caused obvious deterioration in the ultrastructural morphology. Purkinje cells showed irregular contour, shrinked nuclei, and widely dilated rough ER cristae. This evidence of endoplasmic stress may be involved in the degeneration of Purkinje cells (Figure 4A-iii). Moreover, the same group displayed darker granule cells with clumps of heterochromatin (Figure 4B-iii), demyelinated axons in molecular layer (Figure 5A-iii). Activated microglial cells in this group displayed features of pyroptosis, including cellular swelling, distorted nuclei, rarified cytoplasm, reduced ramification of the distal processes and ruptured membrane (Figure 5B-iii). Fortunately, in parallel with the histopathological findings of the IMI

TABLE 2 Histological scoring of the cerebellar cortex damage.

	Control	Ber-Lip group	IMI group	IMI+ Ber-Lip group
Purkinje cells damage/loss	−	−	+++	+
Brain matrix edema	−	−	++	−
Glial cells infiltrates	−	−	++	−

Note: −, Nil; +, Mild records in <15% of examined tissue sections; ++, Moderate records in 16%–35% of examined tissue sections; +++ Sever records in >35% of examined tissue section.

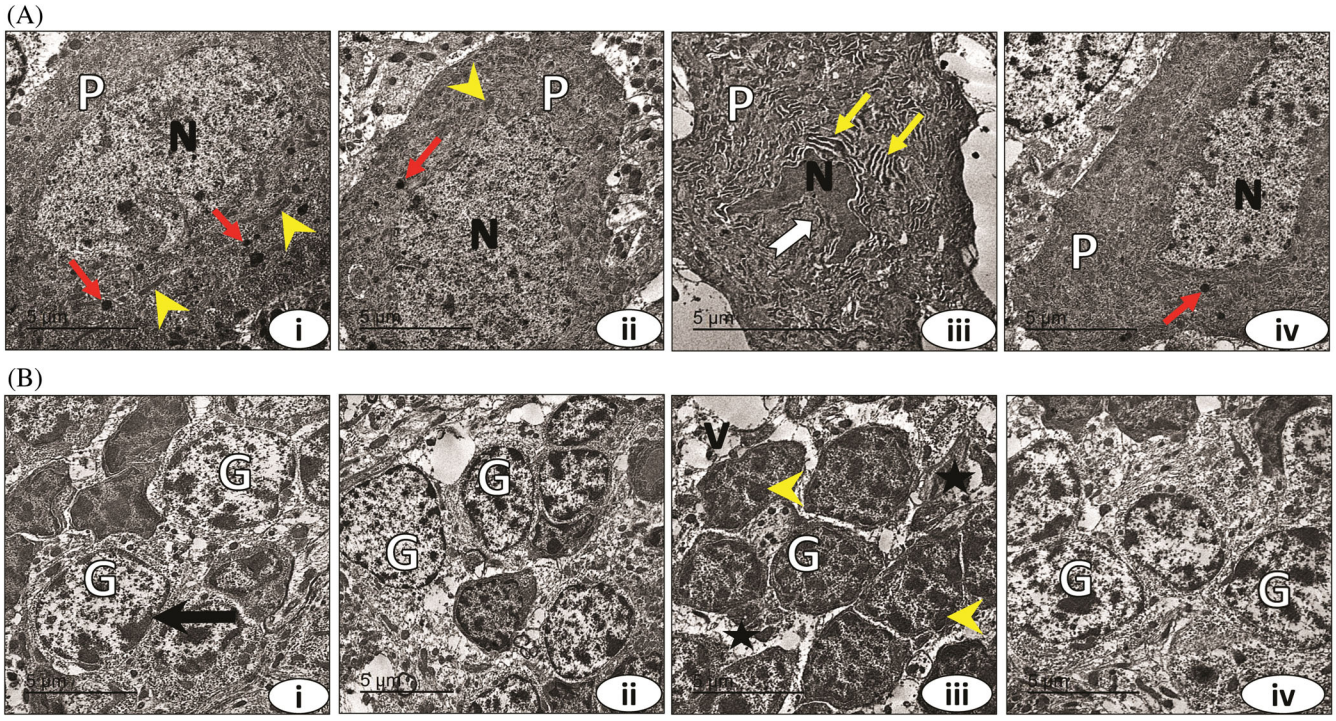

FIGURE 4 Set of electron micrographs representing cerebellar cortices layers of different experimental groups: (A): Purkinje cells layer: (i) Control group: normal large Purkinje cell (P) with large euchromatic oval nucleus (N) displayed almost normal contour. The cytoplasm shows elongated mitochondria (arrowheads) and electron-dense lysosomes (red arrows). (ii) Ber-Lip group: Purkinje cells show the same histological morphology as the control group. (iii) IMI group: signs of degeneration appeared; distorted histological morphology of Purkinje cell, irregular shrunken nucleus (N) with obvious indentation (white arrow), and widely dilated rER (yellow arrows) as sign of pyroptosis. (iv) IMI+ Ber-Lip group: Purkinje cells appeared with improved histological morphology. (B) Granular cells layer: showing (i) Control group: showed normal granule cells (G) with mostly rounded large nuclei surrounded with small rims of cytoplasm (arrow). The surrounding neuropil appeared normal with normal small neuroglia cells. (ii) Ber-Lip group: showed the same morphology as control group. (iii) IMI group: after intoxification, the granule cells (G) appeared with signs of apoptosis. The nuclei are pyknotic with increased clumping of heterochromatin (yellow arrowheads), the surrounding neuropil appeared vacuolated (v) and filled with debris (star). (iv) IMI+ Ber-Lip group: the granule cells appeared relatively normal (scale bar = 5 μm).

+ Ber-Lip group, Ber-Lip alleviated the toxicity of IMI. This group showed improved ultrastructure of Pukinje cells which displayed nearly normal morphology (Figure 4A-iv), granule cells and molecular layer also showed improved morphology (Figures 4B-iv and 5A-iv), respectively. Microglial cells appeared with no features of pyroptosis (Figure 5B-iv). This inhibited pyroptosis of microglial cell positively protected neuronal cell death affecting Purkinje cell.

3.4 | Impact of IMI exposure and Ber-Lip treatment on oxidative stress related parameters

Malondialdehyde, an end-metabolite and sensitive indicator of lipid peroxidation and oxidative damage, was significantly elevated in the IMI group compared to the control. In addition, a substantial decline in GSH level and SOD activity was also demonstrated in

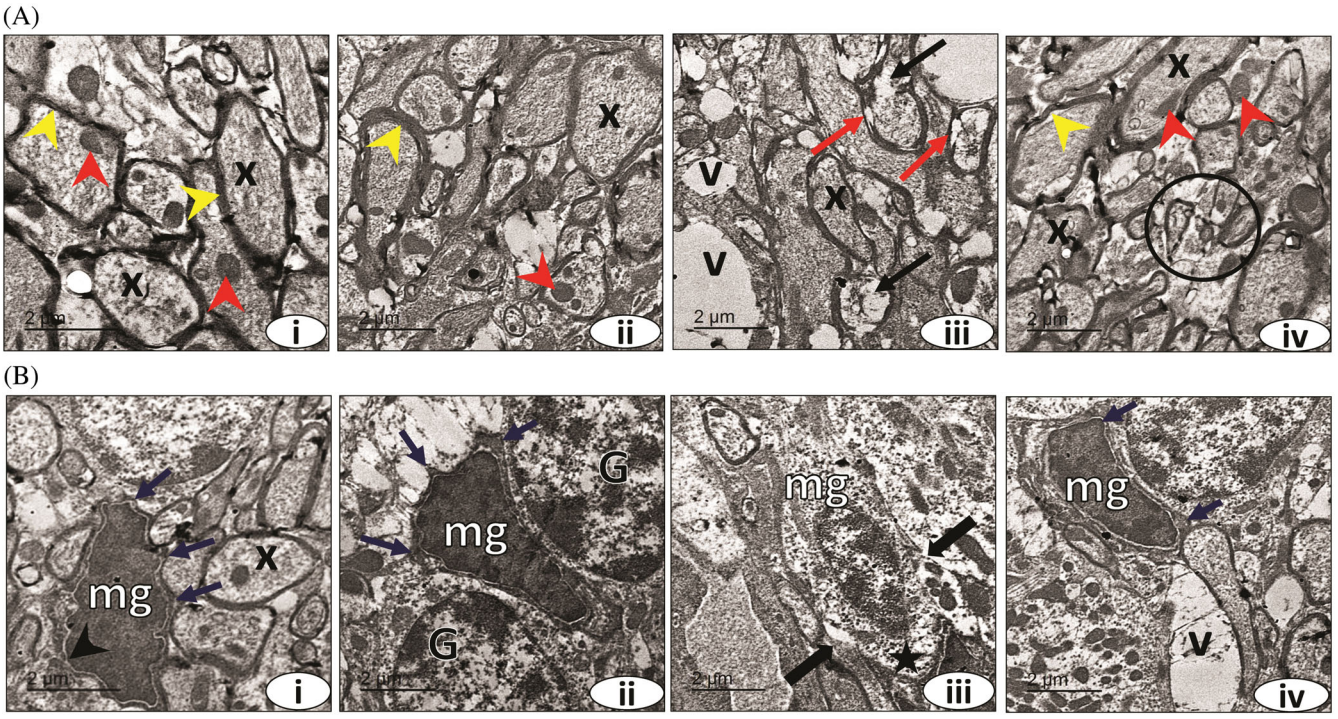

FIGURE 5 Set of electron micrographs representing cerebellar cortices of different experimental groups: (A) Molecular layer: showing (i) control group: most nerve axons (x) are healthy with normal mitochondria (red arrowheads) and surrounded by compact myelin sheathes (yellow arrowheads). (ii) Ber-Lip group: showing the same normal histological features as control group. (iii) IMI group: most of nerve axons (x) are distorted (black arrows) and surrounded by destructed myelin sheaths (red arrows). The surrounding areas are showing vacuolization (v). (iv) IMI+ Ber-Lip group: showed restored histological appearance. But some nerve fibers are atrophied (circle). (B) Microglial cells: (i) Control group: healthy microglial cell (mg) between myelinated nerve axons (x). The microglia showing normal dense nuclei surrounded by normal nuclear membrane (black arrowheads), multiple side processes (blue arrows) and scanty cytoplasm. (ii) Ber-Lip group: Showing the same normal histological features (iii) IMI group: microglia showing pyroptotic feature. The cells are swollen with distorted nuclei, rarified cytoplasm (star), decreased nuclear density and less cellular processes. The cell membrane appeared ruptured (thick arrows). (iv) IMI+ Ber-Lip group: microglial cells appeared nearly normal with dense nuclei and scanty cytoplasm. The surrounding neuropil still showing vacuolated areas (v) (scale bar = 2 µm).

the IMI group compared to the control, indicating a reduced antioxidant capacity in the cerebellar tissue with IMI exposure. Meanwhile, Ber-Lip administration significantly reduced MDA levels while raising GSH concentration and SOD activity in the IMI + Ber-Lip group compared to the IMI group (Figure 6A–C).

3.5 | IMI exposure triggered microglia activation and polarization to the M1 and Ber-Lip treatment skewed the polarity to the M2 phenotype

The results of qPCR revealed that the mRNA expression of M1 phenotype markers CD86 and iNOS were significantly upregulated in the IMI group compared to other groups (Figure 7B,C). In addition, the concentration of M1 type related pro-inflammatory cytokine IL1β was also increased (Figure 7D). Meanwhile, immunohistochemistry analysis showed significantly decreased immunoreactivity of the M2 phenotype marker CD163 (Figure 7A-iii) indicating the activation and predominance of M1 phenotype associated with IMI exposure. It was striking that a notable decrease in TNF-α levels was demonstrated in the IMI group compared to other groups despite being a proinflammatory cytokine that should rise in response to an increase in M1(Figure 7E). There is conflicting evidence on TNF-α role in the context of brain insults and it is unclear whether its effect is protective or toxic hence, more investigations are needed to better understand its cell specific roles.

Ber-Lip treatment was a potent inducer for microglial polarization to the M2 phenotype indicated by the significant downregulation of CD86 and iNOS mRNA expression (Figure 7B,C), decreased IL1β concentration (Figure 7D) and increased

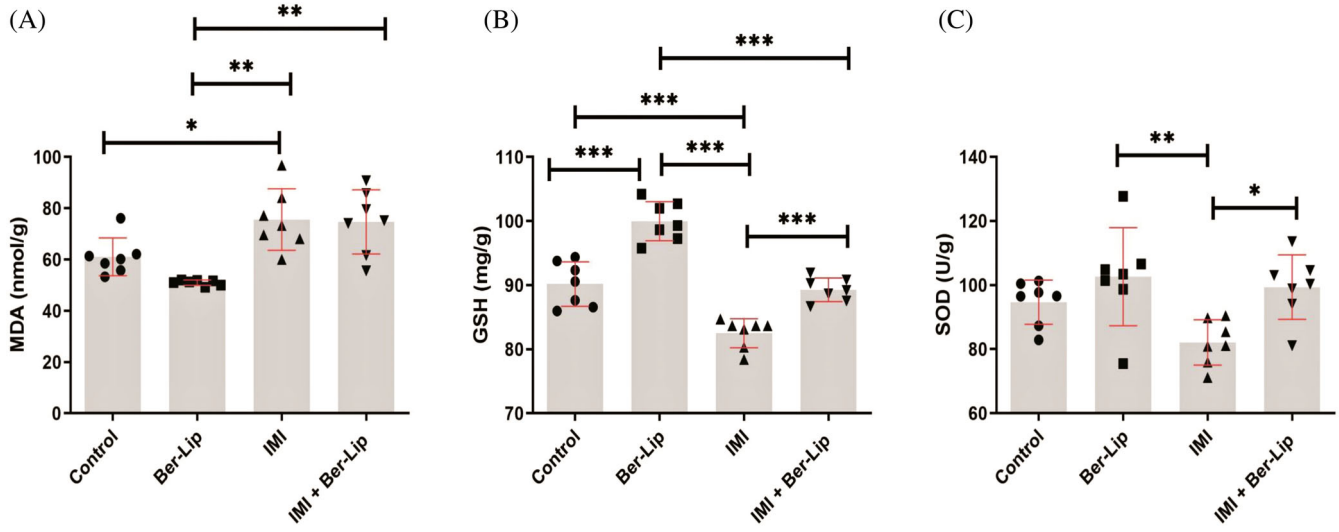

FIGURE 6 Bar–dot plots showing the values of the oxidative stress related parameters for different groups ($n = 7$/group). (A) MDA. (B) GSH. (C) SOD. Jitter data point are overlaying the bar plot. Each dot represents one experimental unit (rat). Results are expressed as mean ± SD. The significance refers to the differences between respective groups in the parameter using one-way ANOVA followed by multiple comparison test. *<0.05, **<0.01 and ***<0.001. GSH, reduced glutathione; MDA, malondialdehyde; SOD, superoxide dismutase.

immunoreactivity of the M2 phenotype marker CD163 (Figure 7A-iv). Moreover, a substantial increase in the concentration of TNF-α was detected with Ber-Lip treatment in the IMI + Ber-Lip group in comparison to the IMI group (Figure 7E) suggesting a neuroprotective role of TNF-α in this context.

3.6 | IMI exposure induced the canonical caspase-1-dependent pyroptotic pathway and Ber-Lip treatment effectively inhibited it

Pyroptosis has recently garnered a lot of attention in relation to its unique role in inflammation. To determine whether IMI administration triggered the canonical pyroptotic pathway, we evaluated the expression levels of NLRP3, caspase-1, GSDMD, and IL-18. The immunohistochemical analysis of NLRP3 (Figure 8A) and qPCR assessment of caspase-1 (Figure 8B), GSDMD (Figure 8C), and IL-18 (Figure 8D) mRNA expression revealed significantly increased immunoreactivity of NLRP3 and significantly upregulated mRNA expression of caspase-1, GSDMD and IL-18 in the IMI group compared to other groups. Meanwhile, significant reductions in NLRP3 immunoreactivity and significant downregulation of caspase-1, GSDMD, and IL-18 mRNA expression were obvious with Ber-Lip treatment in the IMI + Ber-Lip group in comparison to the IMI group.

3.7 | Impact of IMI exposure and Ber-Lip treatment on Aβ deposits formation and neprilysin mRNA expression

An increasing body of research suggests that elevated brain Aβ levels in AD could be the consequence of upstream issues such as neuroinflammation. To further assess the effect of IMI-induced inflammatory response on the brain amyloid load, we measured the Aβ immunoreactivity and diameter. As shown in Figure 9A-iii,v, the immunohistochemistry analysis showed significantly increased immunoreactivity and diameter of Aβ deposits in the IMI group compared with other groups, while Ber-Lip effectively reduced these values in the IMI + Ber-Lip group compared with the IMI group. We next evaluated Neprilysin mRNA expression to explore whether this increase in the brain amyloid load was due to reduced Aβ degradation. Neprilysin mRNA expression level was substantially downregulated in the IMI group compared with other groups and Ber-Lip treatment remarkably enhanced its mRNA expression in the IMI + Ber-Lip group compared with the IMI group (Figure 9B). These results illustrated the contribution of chronic IMI exposure to the development of AD and the potential therapeutic benefit of Ber-Lip in preventing it.

4 | DISCUSSION

Neonicotinoids were formerly thought to be less harmful to mammals due to their weak BBB penetration and reduced

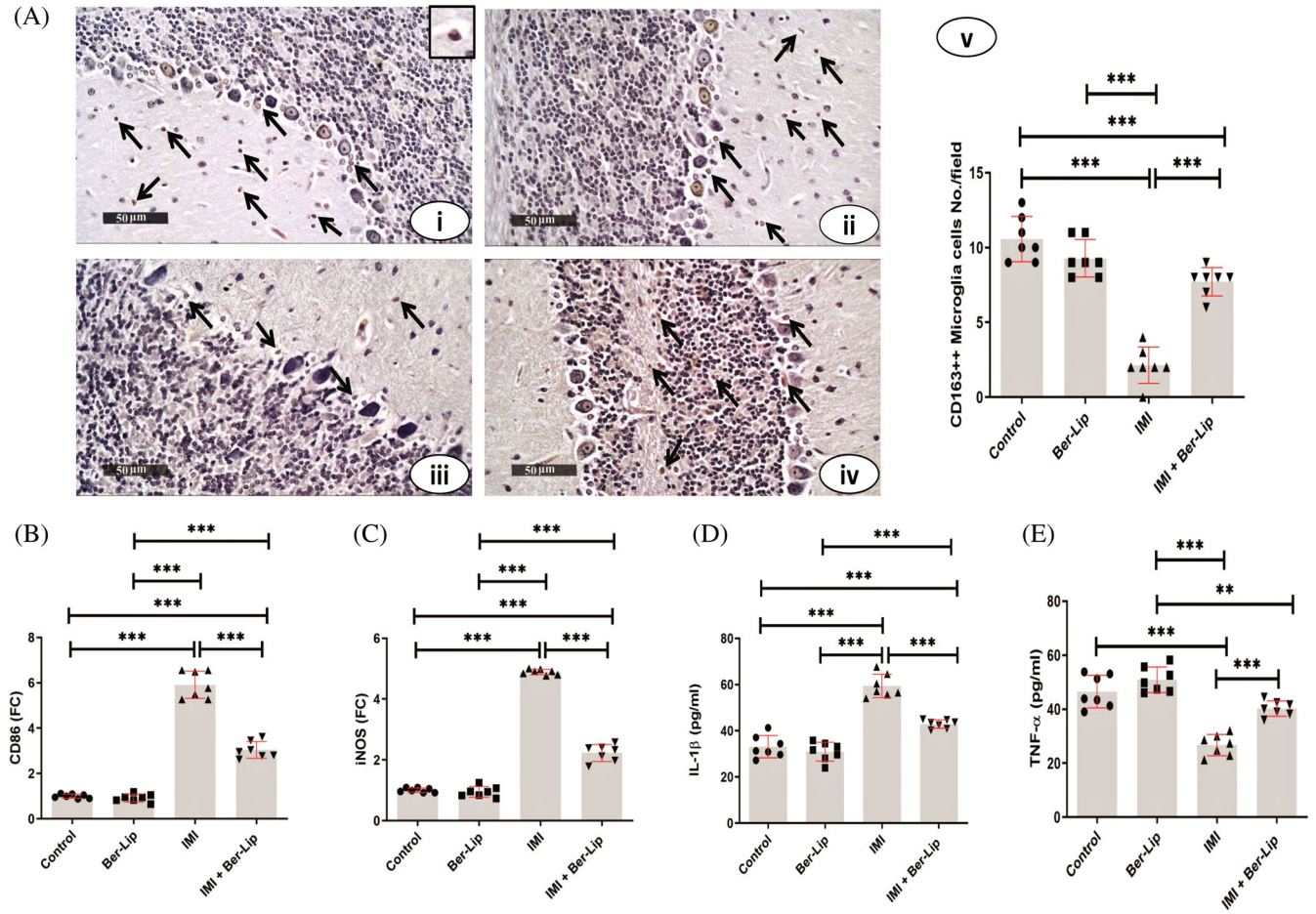

FIGURE 7 Impact of IMI exposure and Ber-Lip treatment on microglia activation and polarization. (A) Set of micrographs representing immunohistochemical analysis of anti-CD163 stained cerebellar cortices from studied groups: (I) Control group and (ii) Ber-Lip group: showing high expression of CD163 positive microglial cells especially in the molecular layer. (iii) IMI group: down-regulated expression of CD163 positive microglial cells. (iv) IMI+ Ber-Lip group: apparent up-regulated expression of CD163 positive microglial cells after treatment (scale bar = 50 µm, magnification = ×400). (v) The histogram represents CD163 positive microglia cells No/field in the experimental groups. (B) mRNA expression of CD 86 and (C) mRNA expression of iNOS. mRNA expression was evaluated in cerebellar tissue samples from experimental groups ($n = 7$/group), as determined by qPCR, normalized for the house-keeping gene B-actin, and expressed relative to controls. Results are expressed as mean ± SD. (D) IL1β and (E) TNF-α levels were evaluated by ELISA in cerebellar tissue samples from the experimental groups ($n = 7$/group). Results are expressed as mean ± SD. *, significant at ($p < 0.05$); **, significant at ($p < 0.01$), and ***, significant at ($p < 0.001$).

affinity for mammalian nAChRs. Due to the widespread acceptance of this theory, the usage of this class of pesticides in contemporary agriculture has increased.

Nevertheless, the findings reported in several studies contradict this notion and demonstrate that these compounds can cross the BBB and that some of their metabolites could have a greater affinity for mammalian nAChRs than the original compound.[2,38,39] Consequently, in this study we aimed to look into possible neurotoxic effect of IMI and the important cellular events that could occur in the cerebellar tissue after its administration.

In this study, the IMI administration triggers changes at both gene, protein and tissue levels making the given rats well discriminated from either the control or Ber-Lip groups. However, administration of Ber-Lip ameriolated most of these changes bringing the levels of these parameters close to the healthy condition (Figure 10), indicating the neuroprotective effect of Ber-Lip in IMI toxified cases. The oxidative stress state was obvious as demonstrated by the significantly increased MDA levels associated with significant lower levels of SOD and GSH in the IMI administered group compared to the control one. These results further support what was previously reported by several studies that established a relationship between NNs induced toxicities and oxidative stress[2,3,40,41] and clearly demonstrates the decrease in the antioxidant capacity represented by the decreased SOD

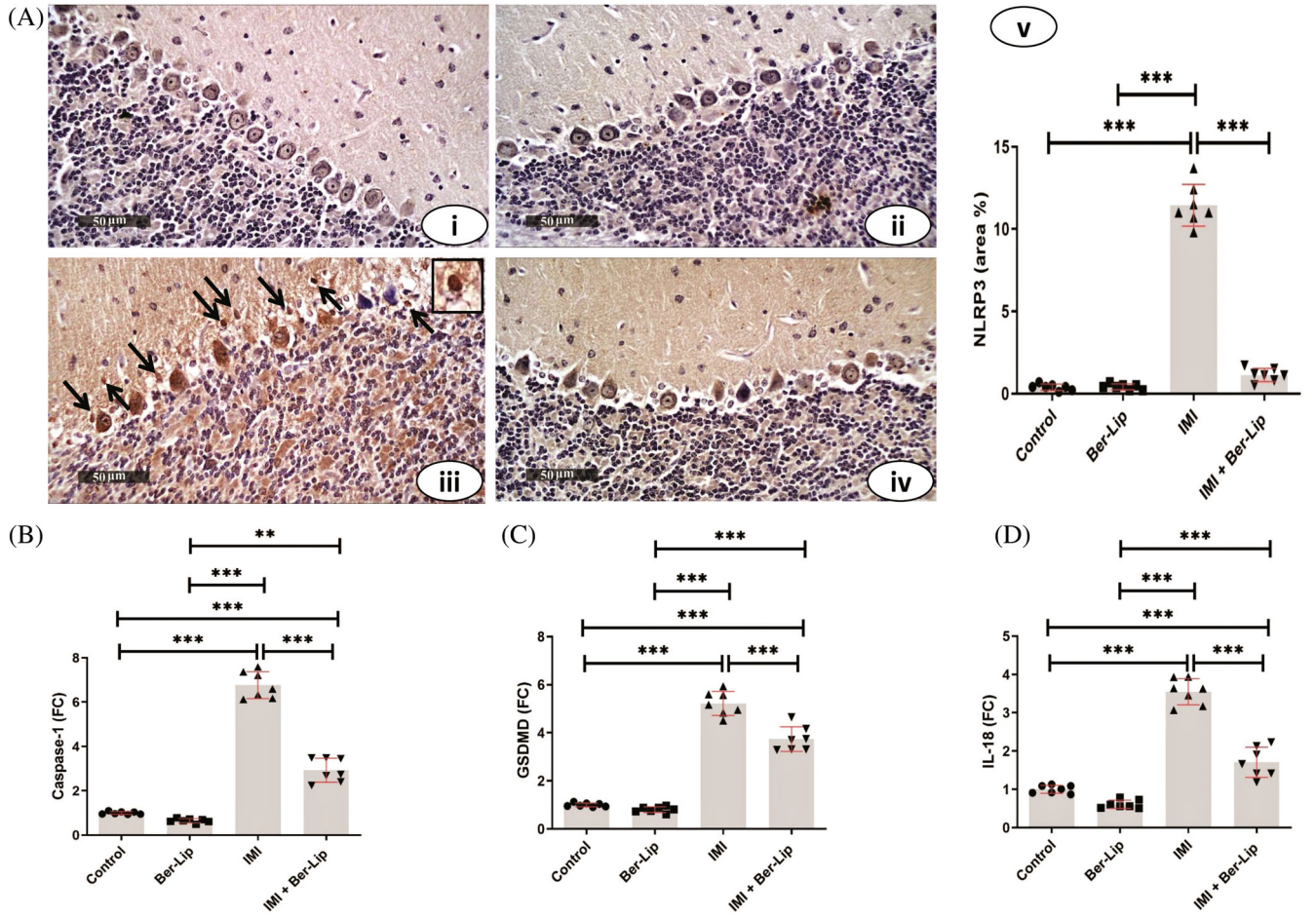

FIGURE 8 Impact of IMI exposure and Ber-Lip treatment on the canonical caspase-1-dependent pyroptotic pathway. (A) Set of micrographs representing immunohistochemical analysis of anti-NLRP3 stained cerebellar cortices from studied groups: (I) Control group and (ii) Ber-Lip group: showing nearly negative expression of NLRP3. (iii) IMI group: High expression of NLRP3 compared to control group. (iv) IMI+ Ber-Lip group: apparent down regulated expression of NLRP3 after treatment (scale bar = 50 µm, magnification = ×400). (v) The histogram represents NLRP3 area % in the experimental groups. mRNA expression of (B) caspase-1, (C) GSDMD and (D) IL-18. mRNA expression was evaluated in cerebellar tissue samples from experimental groups ($n = 7$/group), as determined by qPCR, normalized for the house-keeping gene B-actin, and expressed relative to controls. Results are expressed as mean ± SD. *, significant at ($p < 0.05$); **, significant at ($p < 0.01$) and ***, significant at ($p < 0.001$).

and GSH levels in the IMI treated groups. It is suggested that these antioxidant defense systems attempt to counteract the high ROS production brought on by IMI, these defensive molecular systems get depleted overtime if this overproduction is sustained. Although Duzguner and Erdogan[40] and Katić et al.[3] observed no changes in SOD activity in the brain tissue after IMI administration but the dose they used was much lower than ours.

An important finding of the present study is that IMI triggered microglial activation and polarization to the M1 cytotoxic-proinflammatory phenotype determined by detecting the increased expression of their markers CD86, iNOS and the proinflammatory cytokine IL1β in the IMI-administered group compared to the control. Of note, several studies have displayed the interaction and the crosstalk between reactive microglia and astrocytes in the development of neuroinflammation and elucidated that reactive microglia have the potential to induce the neurotoxic A1 astrocytes phenotype with subsequent promotion of neuroinflammation.[42] Hence, we cannot exclude the role of astrocytes in the contribution to the increased level of proinflammatory cytokines.

Consistent with these results, several previous studies have shown that exposure to NN pesticides polarizes the microglial cells to the M1 cytotoxic phenotype, which could enhance neurotoxicity by inducing excessive release of proinflammatory cytokines.[2,43,44]

Although TNF-α was expected to increase with respect to the observed neurotoxic effect and microglial polarization to the M1; surprisingly, a significant reduction in TNF-α levels was observed in the IMI-intoxicated group compared to the controls. This finding suggests

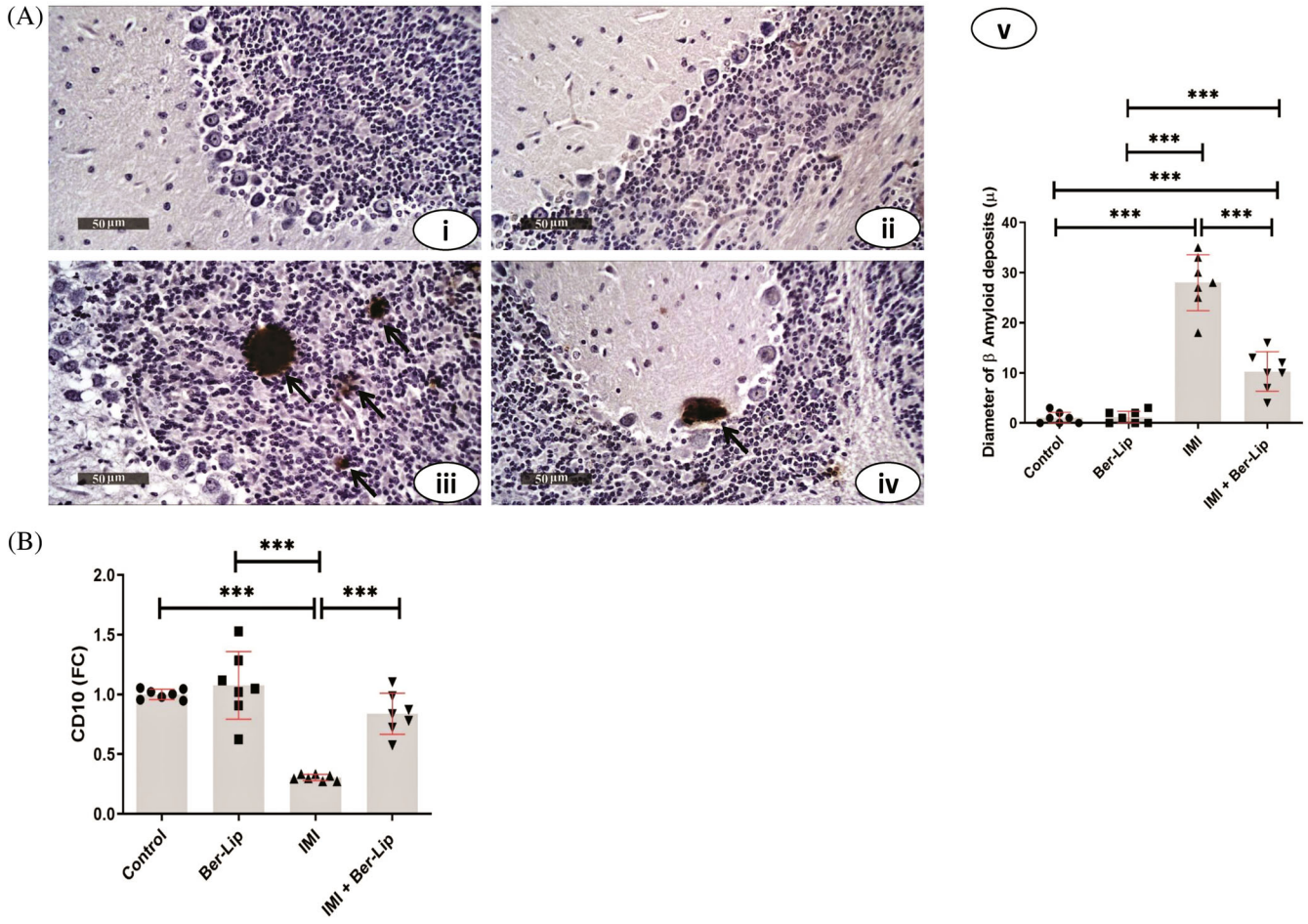

FIGURE 9 Impact of IMI Exposure and Ber-Lip Treatment on Aβ deposits formation and Neprilysin (CD10) mRNA expression. (A) Set of micrographs representing immunohistochemical analysis of anti-β amyloid stained cerebellar cortices from studied groups: (I) Control group and (ii) Ber-Lip group: showing nearly negative expression of β amyloid plaques in all layers of cerebellar cortices. (iii) IMI group: High expression of amyloid plaques. (iv) IMI+ Ber-Lip group: Apparent down regulated expression of anti-β amyloid after treatment (scale bar = 50 µm, magnification = ×400). (v) The histogram represents the diameter of β amyloid deposits (µ) in the experimental groups. (B) mRNA expression of Neprilysin (CD10) in cerebellar tissue samples from experimental groups ($n = 7$/group), as determined by qPCR, normalized for the house-keeping gene B-actin, and expressed relative to controls. Results are expressed as mean ± SD. *, significant at ($p < 0.05$); **, significant at ($p < 0.01$) and ***, significant at ($p < 0.001$).

that one of the mechanisms mediating the neurotoxic effect of IMI is through the reduction of TNF-α levels and further support the findings of several previous reports demonstrated the neuroprotective role of TNF-α.[45–50] Moreover, the decreased SOD and TNF-α levels observed in this study further support what was previously reported by other studies that TNF-α enhances SOD and exerts a protective role through stimulating antioxidant pathways.[46,51]

Although hyper activated microglia play an initiative role in the inflammatory response; the molecular mechanisms that prime microglia to drive the inflammatory response triggered by NN pesticides remain largely unknown. According to recent research, inflammasome-induced microglia pyroptosis is demonstrated to play a crucial role in the pathogenesis of a number of neurological disorders.[52] Canonical pyroptotic death (also called the caspase-1-dependent pathway) is mediated by inflammasome assembly, which is followed by caspase-1 activation. Activated caspase-1 cleaves GSDMD to generate GSDMD-NT fragments which binds to phosphoinositides in the plasma membrane and then generate membrane pores. Additionally, activated caspase-1 catalyzes the maturation of pro-IL-18 and pro-IL1β into IL-18 and IL1β, respectively, which, once being released into the extracellular matrix, trigger inflammatory reactions.

Given the over activation of microglia and the increment in inflammatory cytokines after IMI administration as found in this and other previous studies, we proposed that the overactivated microglia may undergo pyroptosis

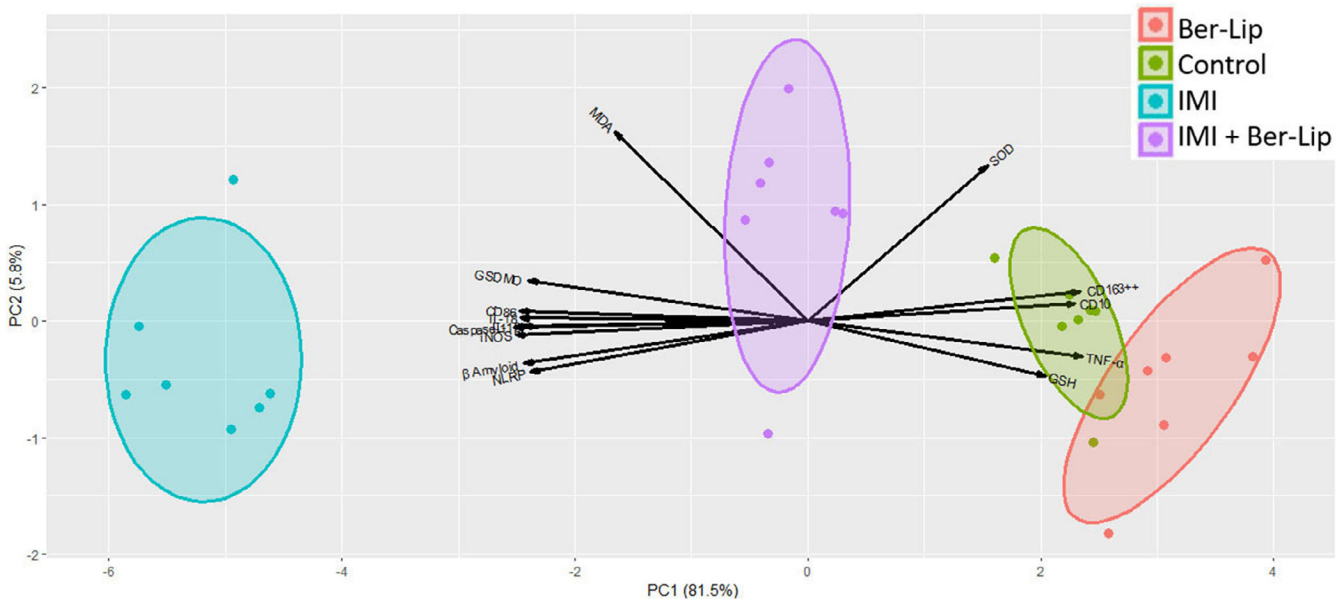

FIGURE 10 Biplot showing the clustering among various groups and the projection of parameters. Each dot refers to one rat and the groups are color-based. The Ellipses around the dots show the confidence intervals and the arrows refer to the analyzed variables.

after IMI administration and aggravates the subsequent inflammation in the brain. To investigate this hypothesis, we evaluated the expression levels of NLRP3, caspase-1, GSDMD, IL-18, and IL1β to determine whether IMI exposure triggers inflammation through the activation of the Canonical pyroptotic pathway. Our findings revealed intensive pyroptosis in the IMI administered group compared to the control as indicated by the substantial increase in the expression levels of NLRP3, caspase-1, GSDMD, IL-18, and IL1β.

Recently, increasing evidence have suggested a critical role of GSDMD-mediated pyroptosis in some brain insults such as seizures, ischemic stroke and depression[53–55] but no studies investigated this pathway induction with chronic IMI intoxication. Therefore, we provide an evidence that NLRP3 inflammasome-mediated microglia pyroptosis is crucially involved in the development of IMI induced neuroinflammation.

Nowadays, it is generally accepted that one of the main causes of AD is a protracted microglial neuroinflammatory response and that microglial-mediated neuroinflammation precedes Aβ plaque formation and thus could be an early trigger for AD development.[42,56,57] Moreover, the role of pyroptosis in the degenerative diseases has attracted increased research attention.[14] Therefore, we analyzed the presence and the diameter of the Aβ deposits immunohistochemically in the studied groups to determine whether the IMI induced persistent inflammatory stimulus had an impact on the overall size of the Aβ deposits. Remarkably, the present work revealed that Aβ deposits in the IMI group had an overall larger diameter than those in the control; which further support the increasing evidences demonstrated that inflammation and immune signaling may not just be a consequence of protein aggregation in the brain as previously reported,[58–60] but that it actually causes the buildup of aggregates at the earliest stages of the disease process.[61–63] However, it is not known if Aβ aggregation is linked to increased Aβ production or reduced Aβ degradation. Therefore, we proposed that the IMI induced persistent inflammatory stimulus would have an impact on the expression of Neprilysin, being one of the major amyloid-degrading enzyme in the brain.[64–66] Herein, the IMI-intoxicated group demonstrated significantly reduced Neprilysin mRNA expression compared to the controls explaining that the increased Aβ plaques size observed in this group could be related to the reduction in Aβ degradation and suggesting an underlying mechanism to the neurotoxic effect of IMI.

In this study we provide evidence that IMI triggers an oxidative stress state, induces microglia activation and polarization to the M1, enhances the canonical pyroptotic pathway with consequential neuroinflammation, and for the first time, reduces Neprilysin mRNA expression with subsequent Aβ plaques aggregation in the cerebellar tissue. Taken together, results of this study support a hypothesized link between the chronic IMI exposure and the onset and progression of AD.

An important point in this study is that all the previously mentioned findings were demonstrated in the cerebellar tissue. There is conflicting evidence regarding the cerebellum's susceptibility to beta amyloid. Some contend

that until later phases of AD, the cerebellum is mostly resistant to amyloid pathology.[67] Others argue that, in mice models of AD, the cerebellum is affected even in the early stages, resulting in abnormalities in both motor and cognitive functions.[68,69] Therefore, results of this study challenges the earlier notion that the cerebellum is spared in AD and provide evidence that AD-related molecular changes occur in the cerebellum, and may contribute to the symptomatology and pathophysiology of AD.

Recently, much attention has been paid to the neuroprotective and anti-neurodegenerative activities of compounds isolated from natural products with high efficacy and low toxicity. Accumulating evidence indicates that Ber, a natural isoquinoline alkaloid, may act as a promising neuroprotective and anti-neurodegenerative agent. However, the low oral bioavailability of Ber due to its poor solubility and membrane permeability hindered its applications.[19,70] The use of innovative therapeutic nano-delivery systems has facilitated the administration of different active molecules. It has been demonstrated that nanoparticles (NPs) possess the capability to facilitate the transportation of molecules into tissues that are typically challenging to access, including the brain. Several types of NPs have been shown to effectively deliver drugs to neural cells in therapies related to NDs among which are the liposomes.[71] This study used Ber chloride loaded nano-PEGylated liposomes. The PEG polymer was included during liposomes preparation to increase their clinical acceptability and improve the effectiveness.[72]

In this study, Ber-Lip administration exerted an obvious enhancement in the antioxidant capacity as evidenced by the significant decrease in the MDA levels and the substantial increase in the SOD and GSH. This result is in line with what previously reported in several studies on Ber antioxidant effect.[73–75] In addition, Ber effectively reversed microglia polarization status from M1 cytotoxic-proinflammatory phenotype, as demonstrated by the significant decrease in CD86, iNOS, and IL1β, to the M 2 anti-inflammatory phenotype as demonstrated by the increased expression of its marker CD163. ROS has been shown to get involved in the functional and phenotypic regulation of macrophages.[76,77] Hence, it seems that IMI-induced oxidative stress state was the driving force behind macrophage polarization to the M1 cytotoxic phenotype and that Ber antioxidant effect has enhanced the skewing towards M2 phenotype.

Although TNF-α levels were frequently lowered by Berb treatment in previous studies,[21,78,79] a contradictory response was observed in this study where Berb proved protective while elevating TNF-α. Results of this study regarding TNF-α; are consistent with those reports on the beneficial effects of TNF-α and further indicates the complexity of the TNF signaling pathways which need further assessments to better understand the cell-specific roles of TNF-α in response to chronic toxic stimuli.

The neuroprotective effect of Berb in this study was also mediated through its inhibitory effect on the canonical pyroptotic pathway as demonstrated by the substantial decrease in the expression levels of NLRP3, caspase-1, GSDMD, IL-18, and IL1β. In line with this result, Qin et al. reported an inhibitory effect of Berb on NLRP3 inflammasome-mediated neuroinflammation in mice model of depression-like behaviors.[21] Additionally, Huang et al. demonstrated inhibitory effect of Berb on NLRP3 inflammasome activation in Parkinson's disease Model.[80] Contradictory to this result, Li et al. discovered that Berb significantly increased ATP-induced pyroptosis and increased the release of caspase-1, p10, and IL1β in macrophages.[81] Moreover, Chu et al. revealed that Ber could induce pyroptosis in HepG2 cells via activating caspase-1.[82] These apparently conflicting reports imply that the roles of Berb on pyroptosis may vary in different pathological conditions and suggest more research on its effect on pyroptosis in the context of chronic IMI intoxication to further support or contradict our result.

Accumulating evidences suggest that Ber could significantly reduce Aβ peptide production by decreasing the Aβ precursor protein (APP) or modulating its processing by β-secretase (also known as BACE1) and γ-secretase.[83] Herein, we add to the existing knowledge that Berb could also promote Aβ peptide clearance as demonstrated by the significantly increased Neprilysin mRNA expression in the Berb administered group compared to the IMI-intoxicated group, suggesting a novel underlying mechanism to the neuroprotective effect of Berb. This study had some limitations as we used only one concentration of IMI and Ber without exploring dose response relationships, and performed all the assessments only at a single time point.

In summary, we present the experimental data showing that IMI long-term intoxication, in this setting, provoked a neurotoxic effect on the cerebellar tissue primarily through increased oxidative stress, enhanced macrophage skewing to the M1 cytotoxic phenotype, enhanced canonical pyroptotic pathway and decreased Neprilysin mRNA expression with subsequent Aβ plaques aggregation. Together, these findings suggest a potential link between chronic neuroinflammation, brought on by IMI long-term intoxication, and its eventual impact on the development of AD. Furthermore, we have delineated the involved molecular mechanism underlying the neuroprotective effect of Berb against IMI intoxication and its therapeutic potential to combat AD.

AUTHOR CONTRIBUTIONS

Conceptualization: Walaa Bayoumie El Gazzar and Amina A. Farag. Investigation: Walaa Bayoumie El Gazzar, Amina A. Farag, Heba Bayoumi, and Yasmin Mohammed Marei. Formal analysis: Walaa Bayoumie El Gazzar. Biostatistics and figures generation: Mohamed Samir. Writing original draft: Walaa Bayoumie El Gazzar, Heba S. Youssef, Heba Bayoumi, Hala Magdy Anwer. Writing review and editing: Walaa Bayoumie El Gazzar, Amina A. Farag, Shimaa K. Mohamed, Azza M. Marei, Reham M. Abdelfatah, Manal Moustafa Mahmoud, Elshaimaa Ahmed Fahmy Aboelkomsan, and Eman Kamel M. Khalfallah. All authors contributed to the discussion of the results. All authors have read and agreed to the published version of the manuscript.

CONFLICT OF INTEREST STATEMENT

The authors declare no conflict of interest.

ORCID

Walaa Bayoumie El Gazzar https://orcid.org/0000-0001-5172-1105
Amina A. Farag https://orcid.org/0000-0003-3014-9909
Mohamed Samir https://orcid.org/0000-0002-1166-0480
Heba Bayoumi https://orcid.org/0000-0002-0931-452X
Heba S. Youssef https://orcid.org/0000-0002-8267-1718
Shimaa K. Mohamed https://orcid.org/0000-0001-9223-0046
Azza M. Marei https://orcid.org/0000-0001-7959-7927
Reham M. Abdelfatah https://orcid.org/0000-0002-6542-749X
Manal Moustafa Mahmoud https://orcid.org/0000-0002-3948-5514
Elshaimaa Ahmed Fahmy Aboelkomsan https://orcid.org/0009-0006-7113-581X
Hala Magdy Anwer https://orcid.org/0000-0002-1225-1814

REFERENCES

1. Saito H, Furukawa Y, Sasaki T, Kitajima S, Kanno J, Tanemura K. Behavioral effects of adult male mice induced by low-level acetamiprid, imidacloprid, and nicotine exposure in early-life. Front Neurosci. 2023;17:1239808. https://doi.org/10.3389/fnins.2023.1239808
2. Costas-Ferreira C, Faro LRF. Neurotoxic effects of neonicotinoids on mammals: what is there beyond the activation of nicotinic acetylcholine receptors?—a systematic review. Int J Mol Sci. 2021;22(16):8413. https://doi.org/10.3390/ijms22168413
3. Katić A, Kašuba V, Kopjar N, Lovaković BT, Marjanović Čermak AM, Mendaš G, et al. Effects of low-level imidacloprid oral exposure on cholinesterase activity, oxidative stress responses, and primary DNA damage in the blood and brain of male Wistar rats. Chem Biol Interact. 2021;338:109287. https://doi.org/10.1016/j.cbi.2020.109287
4. Annabi E, Ben Salem I, Abid-Essefi S. Acetamiprid, a neonicotinoid insecticide, induced cytotoxicity and genotoxicity in PC12 cells. Toxicol Mech Methods. 2019;29(8):580–6. https://doi.org/10.1080/15376516.2019.1624907
5. Salim S. Oxidative stress and the central nervous system. J Pharmacol Exp Ther. 2017;360(1):201–5. https://doi.org/10.1124/jpet.116.237503
6. Chan AH, Schroder K. Inflammasome signaling and regulation of interleukin-1 family cytokines. J Exp Med. 2020;217(1):e20190314. https://doi.org/10.1084/jem.20190314
7. Akhmetzyanova E, Kletenkov K, Mukhamedshina Y, Rizvanov A. Different approaches to modulation of microglia phenotypes after spinal cord injury. Front Syst Neurosci. 2019;13:37. https://doi.org/10.3389/fnsys.2019.00037
8. Chang Y, Zhu J, Wang D, Li H, He Y, Liu K, et al. NLRP3 inflammasome-mediated microglial pyroptosis is critically involved in the development of post-cardiac arrest brain injury. J Neuroinflammation. 2020;17(1):219. https://doi.org/10.1186/s12974-020-01879-1
9. Zheng D, Liwinski T, Elinav E. Inflammasome activation and regulation: toward a better understanding of complex mechanisms. Cell Discov. 2020;6(1):36. https://doi.org/10.1038/s41421-020-0167-x
10. Hu M, Lin Y, Zhang B, Lu D, Lu Z, Cai W. Update of inflammasome activation in microglia/macrophage in aging and aging-related disease. CNS Neurosci Ther. 2019;25(12):1299–307. https://doi.org/10.1111/cns.13262
11. Yang Y, Wang H, Kouadir M, Song H, Shi F. Recent advances in the mechanisms of NLRP3 inflammasome activation and its inhibitors. Cell Death Dis. 2019;10(2):128. https://doi.org/10.1038/s41419-019-1413-8
12. Sun L, Ma W, Gao W, Xing Y, Chen L, Xia Z, et al. Propofol directly induces caspase-1-dependent macrophage pyroptosis through the NLRP3-ASC inflammasome. Cell Death Dis. 2019;10(8):542. https://doi.org/10.1038/s41419-019-1761-4
13. Liao Y, Wang X, Huang L, Qian H, Liu W. Mechanism of pyroptosis in neurodegenerative diseases and its therapeutic potential by traditional Chinese medicine. Front Pharmacol. 2023;14:1122104. https://doi.org/10.3389/fphar.2023.1122104
14. Zhou J, Qiu J, Song Y, Liang T, Liu S, Ren C, et al. Pyroptosis and degenerative diseases of the elderly. Cell Death Dis. 2023;14(2):94. https://doi.org/10.1038/s41419-023-05634-1
15. Nalivaeva N, Zhuravin I, Turner A. Neprilysin expression and functions in development, ageing and disease. Mech Ageing Dev. 2020;192:111363. https://doi.org/10.1016/j.mad.2020.111363
16. Parbo P, Ismail R, Hansen KV, Amidi A, Mårup FH, Gottrup H, et al. Brain inflammation accompanies amyloid in the majority of mild cognitive impairment cases due to Alzheimer's disease. Brain. 2017;140(7):2002–11. https://doi.org/10.1093/brain/awx120
17. Graykowski D, Kasparian K, Caniglia J, Gritsaeva Y, Cudaback E. Neuroinflammation drives APOE genotype-dependent differential expression of neprilysin. J Neuroimmunol. 2020;346:577315. https://doi.org/10.1016/j.jneuroim.2020.577315

18. Massimi L, Pieroni N, Maugeri L, Fratini M, Brun F, Bukreeva I, et al. Assessment of plaque morphology in Alzheimer's mouse cerebellum using three-dimensional X-ray phase-based virtual histology. Sci Rep. 2020;10(1):11233. https://doi.org/10.1038/s41598-020-68045-8
19. Wang M, Xu R, Liu X, Zhang L, Qiu S, Lu Y, et al. A co-crystal berberine-ibuprofen improves obesity by inhibiting the protein kinases TBK1 and IKKε. Commun Biol. 2022;5(1):807. https://doi.org/10.1038/s42003-022-03776-0
20. Kim M, Kim TW, Kim CJ, Shin MS, Hong M, Park HS, et al. Berberine ameliorates brain inflammation in poloxamer 407-induced hyperlipidemic rats. Int Neurourol J. 2019;23-(Suppl 2):S102–10. https://doi.org/10.5213/inj.1938216.108
21. Qin Z, Shi DD, Li W, Cheng D, Zhang YD, Zhang S, et al. Berberine ameliorates depression-like behaviors in mice via inhibiting NLRP3 inflammasome-mediated neuroinflammation and preventing neuroplasticity disruption. J Neuroinflammation. 2023;20(1):54. https://doi.org/10.1186/s12974-023-02744-7
22. Mirhadi E, Rezaee M, Malaekeh-Nikouei B. Nano strategies for berberine delivery, a natural alkaloid of berberis. Biomed Pharmacother. 2018;104:465–73. https://doi.org/10.1016/j.biopha.2018.05.067
23. Abd El-Emam MM, Mostafa M, Farag AA, Youssef HS, El-Demerdash AS, Bayoumi H, et al. The potential effects of quercetin-loaded nanoliposomes on amoxicillin/clavulanate-induced hepatic damage: targeting the SIRT1/Nrf2/NF-κB signaling pathway and microbiota modulation. Antioxidants. 2023;12(8):1487. https://doi.org/10.3390/antiox12081487
24. Salem GA, Mohamed AAR, Khater SI, Noreldin AE, Alosaimi M, Alansari WS, et al. Enhancement of biochemical and genomic pathways through lycopene-loaded nano-liposomes: alleviating insulin resistance, hepatic steatosis, and autophagy in obese rats with non-alcoholic fatty liver disease: involvement of SMO, GLI-1, and PTCH-1 genes. Gene. 2023;883:147670. https://doi.org/10.1016/j.gene.2023.147670
25. Tang L, Li K, Zhang Y, Li H, Li A, Xu Y, et al. Quercetin liposomes ameliorate streptozotocin-induced diabetic nephropathy in diabetic rats. Sci Rep. 2020;10(1):2440. https://doi.org/10.1038/s41598-020-59411-7
26. Khater SI, Almanaa TN, Fattah DMA, Khamis T, Seif MM, Dahran N, et al. Liposome-encapsulated berberine alleviates liver injury in type 2 diabetes via promoting AMPK/mTOR-mediated autophagy and reducing ER stress: morphometric and immunohistochemical scoring. Antioxidants. 2023;12(6):1220. https://doi.org/10.3390/antiox12061220
27. National Research Council. Guide for the care and use of laboratory animals. 8th ed. Washington, DC: The National Academies Press; 2011.
28. Mikolić A, Karačonji IB. Imidacloprid as reproductive toxicant and endocrine disruptor: investigations in laboratory animals. Arch Ind Hyg Toxicol. 2018;69(2):103–8. https://doi.org/10.2478/aiht-2018-69-3144
29. World Health Organization. The WHO Recommended Classification of Pesticides by Hazard and Guidelines to Classification, 2019 edition. Geneva: World Health Organization; 2020.
30. Livak KJ, Schmittgen TD. Analysis of relative gene expression data using real-time quantitative PCR and the $2^{-\Delta\Delta CT}$ method. Methods. 2001;25(4):402–8. https://doi.org/10.1006/meth.2001.1262
31. Bancroft JD, Layton C. The hematoxylin and eosin stain. In: Suvarna SK, Layton C, Bancroft JD, editors. Bancroft's theory and practice of histological techniques. 10th ed. Amsterdam: Elsevier; 2019.
32. Mondal SK. Manual of Histological Techniques. 2nd ed. India: JAYPEE BROTHERS Medical Publishers; 2017. p. 107–22.
33. Mohamed SK, Ahmed AAE, Elkhoely A. Sertraline pretreatment attenuates hemorrhagic transformation induced in rats after cerebral ischemia reperfusion via down regulation of neuronal CD163: involvement of M1/M2 polarization interchange and inhibiting autophagy. J Neuroimmune Pharmacol. 2023;18(4):657–73. https://doi.org/10.1007/s11481-023-10093-8
34. Bozzola JJ. Conventional specimen preparation techniques for transmission electron microscopy. In: Kou J, editor. Electron microscopy: methods and protocols. 3rd ed. United States: Humana Press; 2014. p. 1–19. https://doi.org/10.1007/978-1-62703-776-1_1
35. One-way ANOVA followed by Dunnett's multiple comparisons test was performed using GraphPad Prism version 8.0.0 for Windows, GraphPad Software, Boston, MA. www.graphpad.com
36. Wickham H. Ggplot2. New York: Springer; 2009. https://doi.org/10.1007/978-0-387-98141-3
37. Vu VQ, Friendly M. ggbiplot: a grammar of graphics implementation of biplots. 2024 https://cran.r-project.org/web/packages/ggbiplot/index.html
38. Laubscher B, Diezi M, Renella R, Mitchell EAD, Aebi A, Mulot M, et al. Multiple neonicotinoids in children's cerebro-spinal fluid, plasma, and urine. Environ Health. 2022;21(1):10. https://doi.org/10.1186/s12940-021-00821-z
39. Bhatta OP, Chand S, Chand H, Poudel RC, Lamichhane RP, Singh AK, et al. Imidacloprid poisoning in a young female: a case report. J Med Case Rep. 2023;17(1):43. https://doi.org/10.1186/s13256-022-03742-8
40. Duzguner V, Erdogan S. Chronic exposure to imidacloprid induces inflammation and oxidative stress in the liver & central nervous system of rats. Pestic Biochem Physiol. 2012;104(1):58–64. https://doi.org/10.1016/j.pestbp.2012.06.011
41. Abd-Elhakim YM, Mohammed HH, Mohamed WAM. Imidacloprid impacts on neurobehavioral performance, oxidative stress, and apoptotic events in the brain of adolescent and adult rats. J Agric Food Chem. 2018;66(51):13513–24. https://doi.org/10.1021/acs.jafc.8b05793
42. Gao C, Jiang J, Tan Y, Chen S. Microglia in neurodegenerative diseases: mechanism and potential therapeutic targets. Signal Transduct Target Ther. 2023;8(1):359. https://doi.org/10.1038/s41392-023-01588-0
43. Nakayama A, Yoshida M, Kagawa N, Nagao T. The neonicotinoids acetamiprid and imidacloprid impair neurogenesis and alter the microglial profile in the hippocampal dentate gyrus of mouse neonates. J Appl Toxicol. 2019;39(6):877–87. https://doi.org/10.1002/jat.3776
44. Hassanen EI, Issa MY, Hassan NH, Ibrahim MA, Fawzy IM, Fahmy SA, et al. Potential mechanisms of imidacloprid-induced neurotoxicity in adult rats with attempts on protection using *Origanum majorana* L. oil/extract: in vivo and in silico

studies. ACS Omega. 2023;8(21):18491–508. https://doi.org/10.1021/acsomega.2c08295
45. Zhang XM, Zheng XY, Sharkawi S, Ruan Y, Amir N, Azimullah S, et al. Possible protecting role of TNF-α in kainic acid-induced neurotoxicity via Down-regulation of NFκB signaling pathway. Curr Alzheimer Res. 2013;10(6):660–9. https://doi.org/10.2174/15672050113109990007
46. Bruce AJ, Boling W, Kindy MS, Peschon J, Kraemer PJ, Carpenter MK, et al. Altered neuronal and microglial responses to excitotoxic and ischemic brain injury in mice lacking TNF receptors. Nat Med. 1996;2(7):788–94. https://doi.org/10.1038/nm0796-788
47. Orellana DI, Quintanilla RA, Maccioni RB. Neuroprotective effect of TNFα against the β-amyloid neurotoxicity mediated by CDK5 kinase. Biochim Biophys Acta Mol Cell Res. 2007;1773(2):254–63. https://doi.org/10.1016/j.bbamcr.2006.10.010
48. Barger SW, Hörster D, Furukawa K, Goodman Y, Krieglstein J, Mattson MP. Tumor necrosis factors alpha and beta protect neurons against amyloid beta-peptide toxicity: evidence for involvement of a kappa B-binding factor and attenuation of peroxide and Ca2+ accumulation. Proc Natl Acad Sci U S A. 1995;92(20):9328–32. https://doi.org/10.1073/pnas.92.20.9328
49. Pentón-Rol G, Cervantes-Llanos M, Martínez-Sánchez G, Cabrera-Gómez JA, Valenzuela-Silva CM, Ramírez-Nuñez O, et al. TNF-α and IL-10 downregulation and marked oxidative stress in Neuromyelitis optica. J Inflamm. 2009;6(1):18. https://doi.org/10.1186/1476-9255-6-18
50. Chadwick W, Magnus T, Martin B, Keselman A, Mattson MP, Maudsley S. Targeting TNF-α receptors for neurotherapeutics. Trends Neurosci. 2008;31(10):504–11. https://doi.org/10.1016/j.tins.2008.07.005
51. Warner BB, Burhans MS, Clark JC, Wispe JR. Tumor necrosis factor-alpha increases Mn-SOD expression: protection against oxidant injury. Am J Physiol Cell Mol Physiol. 1991;260(4):L296–301. https://doi.org/10.1152/ajplung.1991.260.4.L296
52. Wu X, Wan T, Gao X, Fu M, Duan Y, Shen X, et al. Microglia pyroptosis: a candidate target for neurological diseases treatment. Front Neurosci. 2022;16:922331. https://doi.org/10.3389/fnins.2022.922331
53. Li S, Sun Y, Song M, Song Y, Fang Y, Zhang Q, et al. NLRP3/caspase-1/GSDMD-mediated pyroptosis exerts a crucial role in astrocyte pathological injury in mouse model of depression. JCI Insight. 2021;6(23):e146852. https://doi.org/10.1172/jci.insight.146852
54. Wang K, Sun Z, Ru J, Wang S, Huang L, Ruan L, et al. Ablation of GSDMD improves outcome of ischemic stroke through blocking canonical and non-canonical inflammasomes dependent pyroptosis in microglia. Front Neurol. 2020;11:577927. https://doi.org/10.3389/fneur.2020.577927
55. Xia L, Liu L, Cai Y, Zhang Y, Tong F, Wang Q, et al. Inhibition of gasdermin D-mediated pyroptosis attenuates the severity of seizures and astroglial damage in kainic acid-induced epileptic mice. Front Pharmacol. 2022;12:751644. https://doi.org/10.3389/fphar.2021.751644
56. Long HZ, Zhou ZW, Cheng Y, Luo HY, Li FJ, Xu SG, et al. The role of microglia in Alzheimer's disease from the perspective of immune inflammation and iron metabolism. Front Aging Neurosci. 2022;14:888989. https://doi.org/10.3389/fnagi.2022.888989
57. Zhang W, Xiao D, Mao Q, Xia H. Role of neuroinflammation in neurodegeneration development. Signal Transduct Target Ther. 2023;8(1):267. https://doi.org/10.1038/s41392-023-01486-5
58. Blasko I, Stampfer-Kountchev M, Robatscher P, Veerhuis R, Eikelenboom P, Grubeck-Loebenstein B. How chronic inflammation can affect the brain and support the development of Alzheimer's disease in old age: the role of microglia and astrocytes. Aging Cell. 2004;3(4):169–76. https://doi.org/10.1111/j.1474-9728.2004.00101.x
59. Yap JKY, Pickard BS, Chan EWL, Gan SY. The role of neuronal NLRP1 inflammasome in Alzheimer's disease: bringing neurons into the neuroinflammation game. Mol Neurobiol. 2019;56(11):7741–53. https://doi.org/10.1007/s12035-019-1638-7
60. Han C, Yang Y, Guan Q, Zhang X, Shen H, Sheng Y, et al. New mechanism of nerve injury in Alzheimer's disease: β-amyloid-induced neuronal pyroptosis. J Cell Mol Med. 2020;24(14):8078–90. https://doi.org/10.1111/jcmm.15439
61. Hong S, Beja-Glasser VF, Nfonoyim BM, Frouin A, Li S, Ramakrishnan S, et al. Complement and microglia mediate early synapse loss in Alzheimer mouse models. Science. 2016;352(6286):712–6. https://doi.org/10.1126/science.aad8373
62. Sosna J, Philipp S, Albay R, Reyes-Ruiz JM, Baglietto-Vargas D, LaFerla FM, et al. Early long-term administration of the CSF1R inhibitor PLX3397 ablates microglia and reduces accumulation of intraneuronal amyloid, neuritic plaque deposition and pre-fibrillar oligomers in 5XFAD mouse model of Alzheimer's disease. Mol Neurodegener. 2018;13(1):11. https://doi.org/10.1186/s13024-018-0244-x
63. Shi Q, Chowdhury S, Ma R, le KX, Hong S, Caldarone BJ, et al. Complement C3 deficiency protects against neurodegeneration in aged plaque-rich APP/PS1 mice. Sci Transl Med. 2017;9(392):eaaf6295. https://doi.org/10.1126/scitranslmed.aaf6295
64. Rofo F, Metzendorf NG, Saubi C, Suominen L, Godec A, Sehlin D, et al. Blood–brain barrier penetrating neprilysin degrades monomeric amyloid-beta in a mouse model of Alzheimer's disease. Alzheimers Res Ther. 2022;14(1):180. https://doi.org/10.1186/s13195-022-01132-2
65. Iwata N, Tsubuki S, Takaki Y, Watanabe K, Sekiguchi M, Hosoki E, et al. Identification of the major Aβ1–42-degrading catabolic pathway in brain parenchyma: suppression leads to biochemical and pathological deposition. Nat Med. 2000;6(2):143–50. https://doi.org/10.1038/72237
66. Iwata N, Tsubuki S, Takaki Y, Shirotani K, Lu B, Gerard NP, et al. Metabolic regulation of brain Aβ by neprilysin. Science. 2001;292(5521):1550–2. https://doi.org/10.1126/science.1059946
67. Liang KJ, Carlson ES. Resistance, vulnerability and resilience: a review of the cognitive cerebellum in aging and neurodegenerative diseases. Neurobiol Learn Mem. 2020;170:106981. https://doi.org/10.1016/j.nlm.2019.01.004
68. Hoxha E, Lippiello P, Zurlo F, Balbo I, Santamaria R, Tempia F, et al. The emerging role of altered cerebellar synaptic processing in Alzheimer's disease. Front Aging Neurosci. 2018;10:396. https://doi.org/10.3389/fnagi.2018.00396
69. Jacobs HIL, Hopkins DA, Mayrhofer HC, Bruner E, van Leeuwen FW, Raaijmakers W, et al. The cerebellum in Alzheimer's disease: evaluating its role in cognitive decline. Brain. 2018;141(1):37–47. https://doi.org/10.1093/brain/awx194
70. Fan D, Liu L, Wu Z, Cao M. Combating neurodegenerative diseases with the plant alkaloid berberine: molecular mechanisms

and therapeutic potential. Curr Neuropharmacol. 2019;17(6):563–79. https://doi.org/10.2174/1570159X16666180419141613
71. Nayab DE, Din F u, Ali H, Kausar WA, Urooj S, Zafar M, et al. Nano biomaterials based strategies for enhanced brain targeting in the treatment of neurodegenerative diseases: an up-to-date perspective. J Nanobiotechnol. 2023;21(1):477. https://doi.org/10.1186/s12951-023-02250-1
72. Taher M, Susanti D, Haris MS, Rushdan AA, Widodo RT, Syukri Y, et al. PEGylated liposomes enhance the effect of cytotoxic drug: a review. Heliyon. 2023;9(3):e13823. https://doi.org/10.1016/j.heliyon.2023.e13823
73. Ibrahim Fouad G, Ahmed KA. Neuroprotective potential of berberine against doxorubicin-induced toxicity in Rat's brain. Neurochem Res. 2021;46(12):3247–63. https://doi.org/10.1007/s11064-021-03428-5
74. Shaker FH, El-Derany MO, Wahdan SA, El-Demerdash E, El-Mesallamy HO. Berberine ameliorates doxorubicin-induced cognitive impairment (chemobrain) in rats. Life Sci. 2021;269:119078. https://doi.org/10.1016/j.lfs.2021.119078
75. Deng H, Jia Y, Pan D, Ma Z. Berberine alleviates rotenone-induced cytotoxicity by antioxidation and activation of PI3K/Akt signaling pathway in SH-SY5Y cells. Neuroreport. 2020;31(1):41–7. https://doi.org/10.1097/WNR.0000000000001365
76. Tan HY, Wang N, Li S, Hong M, Wang X, Feng Y. The reactive oxygen species in macrophage polarization: reflecting its dual role in progression and treatment of human diseases. Oxid Med Cell Longev. 2016;2016:1–16. https://doi.org/10.1155/2016/2795090
77. Morris G, Gevezova M, Sarafian V, Maes M. Redox regulation of the immune response. Cell Mol Immunol. 2022;19(10):1079–101. https://doi.org/10.1038/s41423-022-00902-0
78. Maleki SN, Aboutaleb N, Souri F. Berberine confers neuroprotection in coping with focal cerebral ischemia by targeting inflammatory cytokines. J Chem Neuroanat. 2018;87:54–9. https://doi.org/10.1016/j.jchemneu.2017.04.008
79. Azadi R, Mousavi SE, Kazemi NM, Yousefi-Manesh H, Rezayat SM, Jaafari MR. Anti-inflammatory efficacy of berberine Nanomicelle for improvement of cerebral ischemia: formulation, characterization and evaluation in bilateral common carotid artery occlusion rat model. BMC Pharmacol Toxicol. 2021;22(1):54. https://doi.org/10.1186/s40360-021-00525-7
80. Huang S, Liu H, Lin Y, Liu M, Li Y, Mao H, et al. Berberine protects against NLRP3 inflammasome via ameliorating autophagic impairment in MPTP-induced Parkinson's disease model. Front Pharmacol. 2021;11:618787. https://doi.org/10.3389/fphar.2020.618787
81. Li CG, Yan L, Jing YY, Xu LH, Liang YD, Wei HX, et al. Berberine augments ATP-induced inflammasome activation in macrophages by enhancing AMPK signaling. Oncotarget. 2017;8(1):95–109. https://doi.org/10.18632/oncotarget.13921
82. Chu Q, Jiang Y, Zhang W, Xu C, du W, Tuguzbaeva G, et al. Pyroptosis is involved in the pathogenesis of human hepatocellular carcinoma. Oncotarget. 2016;7(51):84658–65. https://doi.org/10.18632/oncotarget.12384
83. Dan L, Hao Y, Li J, Wang T, Zhao W, Wang H, et al. Neuroprotective effects and possible mechanisms of berberine in animal models of Alzheimer's disease: a systematic review and meta-analysis. Front Pharmacol. 2024;14:1287750. https://doi.org/10.3389/fphar.2023.1287750

How to cite this article: El Gazzar WB, Farag AA, Samir M, Bayoumi H, Youssef HS, Marei YM, et al. Berberine chloride loaded nano-PEGylated liposomes attenuates imidacloprid-induced neurotoxicity by inhibiting NLRP3/Caspase-1/GSDMD-mediated pyroptosis. BioFactors. 2024. https://doi.org/10.1002/biof.2107